Razumov-Stroganov–type Correspondences in the 6-Vertex and $O(1)$ Dense Loop Model

Andrea Sportiello

LIPN – Université Paris Nord,
UMR 7030 CNRS

FPSAC '13

The 25th International Conference
on Formal Power Series
and Algebraic Combinatorics
Paris, France, June 24-28, 2013

Tiling problems ≡ counting solutions to puzzles...

Consider the simplest set of puzzle pieces...

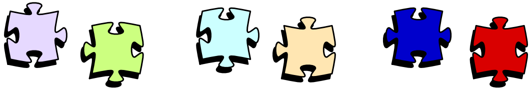

...in how many ways can you tile a $n \times n$ square with these boundary conditions?

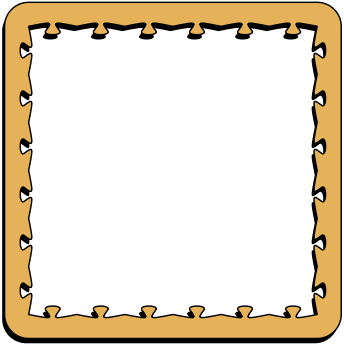

Tiling problems $\equiv$ counting solutions to puzzles...

Consider the simplest set of puzzle pieces...

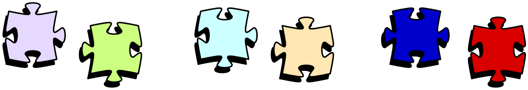

...in how many ways can you tile a $n \times n$ square

with these boundary conditions?

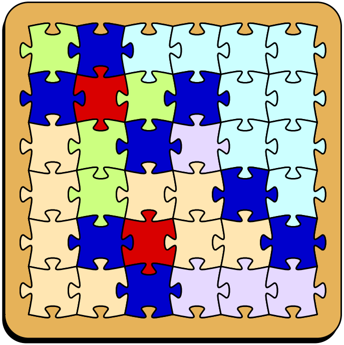

Tiling problems ≡ counting solutions to puzzles. . .

Consider the simplest set of puzzle pieces. . .

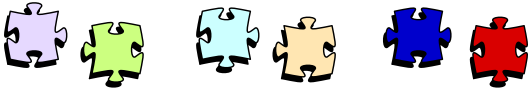

. . . in how many ways can you tile a $n \times n$ square with these boundary conditions?

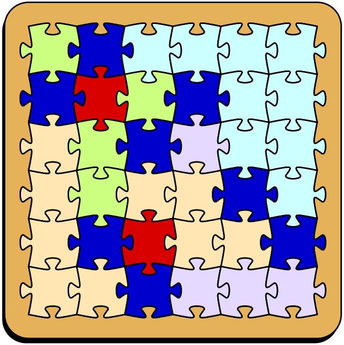

Answer:

n	A_n
1	1
2	2
3	7
4	42
5	429
6	7436

. . .

Some problems are better than others

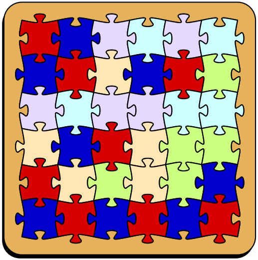

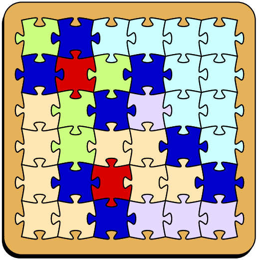

	$\widetilde{A}_n$	n	A_n	
	1	1	1	
	2	2	2	
	7	3	7	
	64	4	42	
	1322	5	429	
	64914	6	7436	

. . .

Some problems are better than others

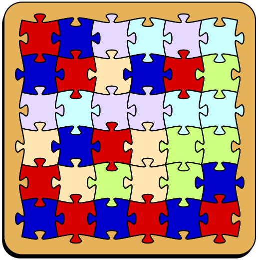

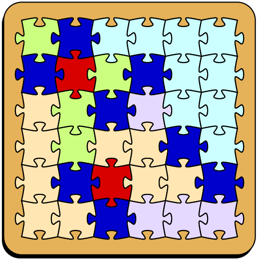

Factorisation	$\widetilde{A}_n$	n	A_n	Factorisation
1	1	1	1	1
2	2	2	2	2
7	7	3	7	7
2^6	64	4	42	$2 \cdot 3 \cdot 7$
$2 \cdot 661$	1322	5	429	$3 \cdot 11 \cdot 13$
$2 \cdot 3 \cdot 31 \cdot 349$	64914	6	7436	$2^2 \cdot 11 \cdot 13^2$

$\cdots$

Some problems are better than others

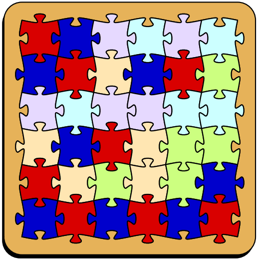

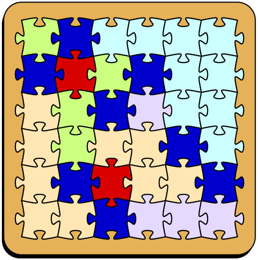

small factors!

In fact

$$A_n = \prod_{j=0}^{n-1} \frac{(3j+1)!}{(n+j)!}$$

Factorisation	$\widetilde{A}_n$	n	A_n	Factorisation
1	1	1	1	1
2	2	2	2	2
7	7	3	7	7
2^6	64	4	42	$2 \cdot 3 \cdot 7$
$2 \cdot 661$	1322	5	429	$3 \cdot 11 \cdot 13$
$2 \cdot 3 \cdot 31 \cdot 349$	64914	6	7436	$2^2 \cdot 11 \cdot 13^2$

...

Some problems are better than others

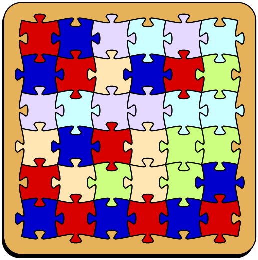

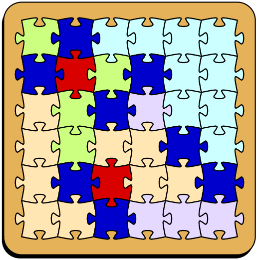

small factors!

In fact

$$A_n = \prod_{j=0}^{n-1} \frac{(3j+1)!}{(n+j)!}$$

Factorisation	$\widetilde{A}_n$	n	A_n	Factorisation
1	1	1	1	1
2	2	2	2	2
7	7	3	7	7
2^6	64	4	42	$2 \cdot 3 \cdot 7$
$2 \cdot 661$	1322	5	429	$3 \cdot 11 \cdot 13$
$2 \cdot 3 \cdot 31 \cdot 349$	64914	6	7436	$2^2 \cdot 11 \cdot 13^2$

$\cdots$

. . . this is a job for

Puzzles and Alternating Sign Matrices

Our puzzles are in bijections with certain matrices

filled with $\{-1, 0, +1\}$ elements.

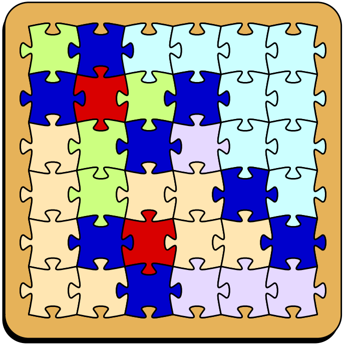

Our puzzles are in bijections with certain matrices
filled with $\{-1, 0, +1\}$ elements.

Forget about color nuances in the four light tiles.
Blue and red pieces must alternate along rows and colours
(they flip back and forth the tile joints).
Boundaries force one more blue than red in each row and column.

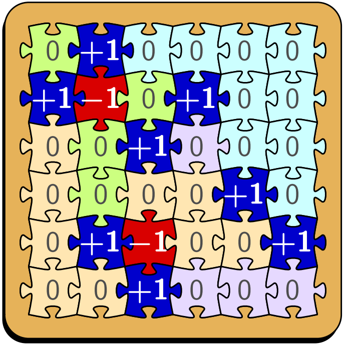

These structures are called
Alternating Sign Matrices

Puzzles and Alternating Sign Matrices

Our puzzles are in bijections with certain matrices filled with $\{-1, 0, +1\}$ elements.

Forget about color nuances in the four light tiles.
Blue and red pieces must alternate along rows and colours (they flip back and forth the tile joints).
Boundaries force one more blue than red in each row and column.

$$\begin{pmatrix} 0 & +1 & 0 & 0 & 0 & 0 \\ +1 & -1 & 0 & +1 & 0 & 0 \\ 0 & 0 & +1 & 0 & 0 & 0 \\ 0 & 0 & 0 & 0 & +1 & 0 \\ 0 & +1 & -1 & 0 & 0 & +1 \\ 0 & 0 & +1 & 0 & 0 & 0 \end{pmatrix}$$

These structures are called Alternating Sign Matrices

Alternating Sign Matrices: some history

Alternating Sign Matrices arose in combinatorics through the work of Mills, Robbins and Rumsey ('80s)... they took the old Dodgson Condensation Algorithm (1866)

$$\det M = \frac{\det M_{1,1} \det M_{n,n} - \det M_{1,n} \det M_{n,1}}{\det M_{1n,1n}}$$

and defined a λ-determinant algorithmically, as

$$\det_\lambda M = \frac{\det_\lambda M_{1,1} \det_\lambda M_{n,n} - \boldsymbol{\lambda} \det_\lambda M_{1,n} \det_\lambda M_{n,1}}{\det_\lambda M_{1n,1n}}$$

The result is (surprisingly) a Laurent polynomial in entries m_{ij}: "old" permutation monomials take a λ^k factor, "new" Laurent monomials have ± 1 exponents coded by the non-trivial ASM's, and have also $(1-\lambda)^h$ factors...

...a 3 × 3 example:

$$\det\ M = m_{11}m_{22}m_{33} + m_{12}m_{23}m_{31} + m_{13}m_{21}m_{32}$$

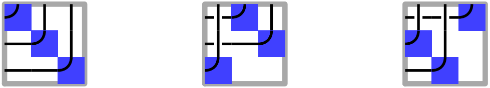

$$- \ m_{11}m_{23}m_{32} - m_{12}m_{21}m_{33} - m_{13}m_{22}m_{31}$$

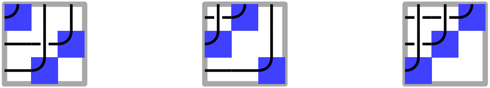

J. Propp: *Lambda-determinants and Domino Tilings*, 2005

...a 3×3 example:

$$\det_{\lambda} M = m_{11} m_{22} m_{33} + \lambda^2 m_{12} m_{23} m_{31} + \lambda^2 m_{13} m_{21} m_{32}$$

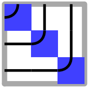
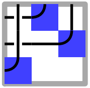
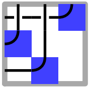

$$-\lambda\, m_{11} m_{23} m_{32} - \lambda\, m_{12} m_{21} m_{33} - \lambda^3 m_{13} m_{22} m_{31}$$

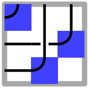
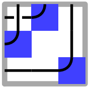
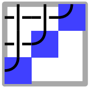

$$-\lambda(1-\lambda)\,\frac{m_{12} m_{21} m_{23} m_{32}}{m_{22}}$$

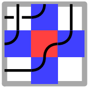

J. Propp: *Lambda-determinants and Domino Tilings*, 2005

Unrestricted Plane Partitions

Take the 3D octant $\mathbb{N}^3$.
Pile cubes (subject to "gravity" along the $(1,1,1)$ axis).
Call $|\pi|$ the number of cubes in π

Generating function
(MacMahon, 1912)

$$\sum_{\pi} q^{|\pi|} = \prod_{j \geq 1} \frac{1}{(1-q^j)^j}$$

Meaningful for $q \in \mathbb{C}$, $|q| < 1$

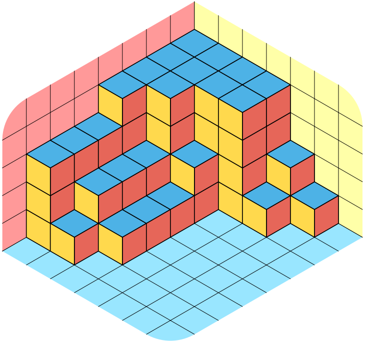

Plane Partitions in a box

In a compact box, can push q to the "combinatorial point" $q = 1$

No symmetry:

P.A. MacMahon (1915)

$$M_{a,b,c} = \prod_{\substack{0\le i<a\\0\le j<b\\0\le k<c}} \frac{i+j+k+2}{i+j+k+1} = \prod_{0\le j<c} \frac{j!(j+a+b)!}{(j+a)!(j+b)!}$$

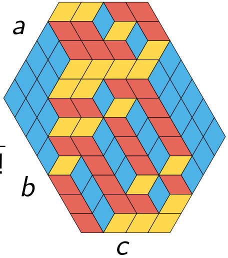

Plane Partitions and Gelfand–Tsetlin patterns

MacMahon 1915's 'boxed' formula is a special case of a formula for lozenge tilings on trapezoids, with generic boundary conditions at the long basis. Configurations in this geometry may look weird, but are in easy bijection with the "*triangular Gelfand–Tsetlin patterns with top row* $\mathbf{x}$" discussed in G. Olshanski talk.

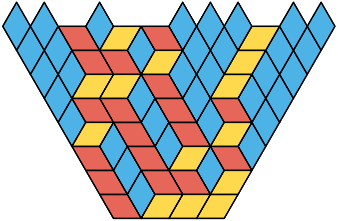

Plane Partitions and Gelfand–Tsetlin patterns

MacMahon 1915's 'boxed' formula is a special case of a formula for lozenge tilings on trapezoids, with generic boundary conditions at the long basis. Configurations in this geometry may look weird, but are in easy bijection with the "*triangular Gelfand–Tsetlin patterns with top row* **x**" discussed in G. Olshanski talk.

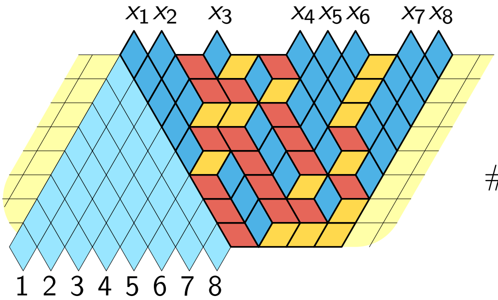

$$\#\mathrm{GT}(\mathbf{x}) = \prod_{i<j} \frac{x_j - x_i}{j - i}$$

Plane Partitions and Gelfand–Tsetlin patterns

MacMahon 1915's 'boxed' formula is a special case of a formula for lozenge tilings on trapezoids, with generic boundary conditions at the long basis. Configurations in this geometry may look weird, but are in easy bijection with the "*triangular Gelfand–Tsetlin patterns with top row* **x**" discussed in G. Olshanski talk.

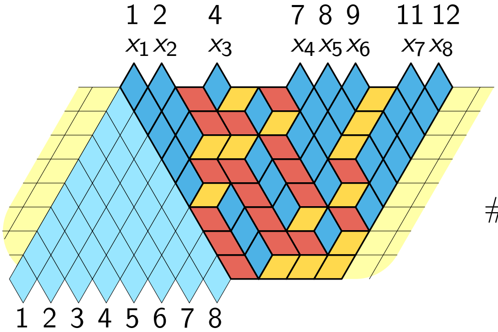

$$\#\mathrm{GT}(\mathbf{x}) = \prod_{i<j} \frac{x_j - x_i}{j - i}$$

Plane Partitions in a box

In a compact box, can push q to the "combinatorial point" $q = 1$

No symmetry:

P.A. MacMahon (1915)

$$M_{a,b,c} = \prod_{\substack{0 \le i < a \\ 0 \le j < b \\ 0 \le k < c}} \frac{i+j+k+2}{i+j+k+1} = \prod_{0 \le j < c} \frac{j!(j+a+b)!}{(j+a)!(j+b)!}$$

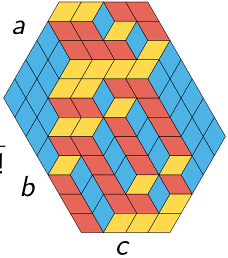

...various symmetry classes...

Maximally symmetric (TSSCPP):

G. Andrews (1994)

$$A_n = \prod_{0 \le j < n} \frac{(3j+1)!}{(n+j)!} = \prod_{0 \le j < n} \frac{j!\,(3j+1)!}{(2j)!(2j+1)!}$$

Plane Partitions in a box

In a compact box, can push q to the "combinatorial point" $q = 1$

No symmetry:

P.A. MacMahon (1915)

$$M_{a,b,c} = \prod_{\substack{0 \le i < a \\ 0 \le j < b \\ 0 \le k < c}} \frac{i+j+k+2}{i+j+k+1} = \prod_{0 \le j < c} \frac{j!(j+a+b)!}{(j+a)!(j+b)!}$$

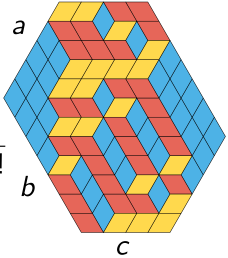

...various symmetry classes...

Maximally symmetric (TSSCPP):

G. Andrews (1994)

$$A_n = \prod_{0 \le j < n} \frac{(3j+1)!}{(n+j)!} = \prod_{0 \le j < n} \frac{j!\,(3j+1)!}{(2j)!(2j+1)!}$$

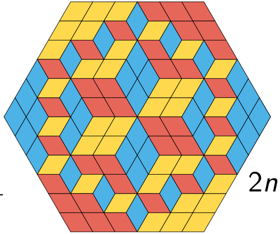

Plane Partitions in a box

In a compact box, can push q to the "combinatorial point" $q = 1$

No symmetry:

P.A. MacMahon (1915)

$$M_{a,b,c} = \prod_{\substack{0 \le i < a \\ 0 \le j < b \\ 0 \le k < c}} \frac{i+j+k+2}{i+j+k+1} = \prod_{0 \le j < c} \frac{j!(j+a+b)!}{(j+a)!(j+b)!}$$

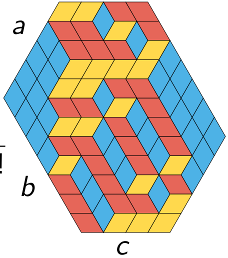

...various symmetry classes...

Maximally symmetric (TSSCPP):

G. Andrews (1994)

$$A_n = \prod_{0 \le j < n} \frac{(3j+1)!}{(n+j)!} = \prod_{0 \le j < n} \frac{j!\,(3j+1)!}{(2j)!(2j+1)!}$$

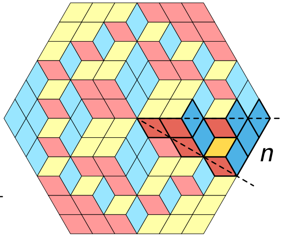

(TSSC) Plane Partitions and Alternating Sign Matrices

You might have noticed the statement of the famous Alternating Sign Matrix Conjecture, posed by Mills, Robbins and Rumsey, and finally solved by Zeilberger, and by Kuperberg, around 1996.

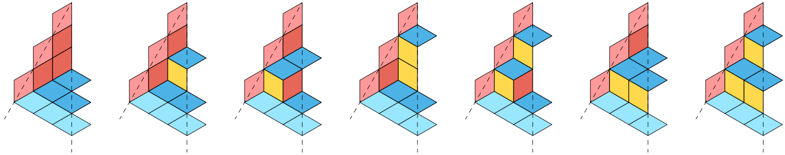

TSSCPP in a hexagon of side $2n$ = # ASM in a square of side n

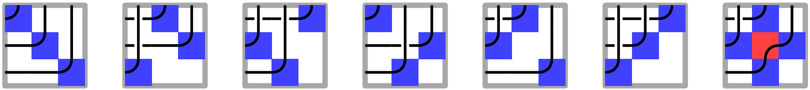

D.M. Bressoud and J. Propp, *How the Alternating Sign Matrix Conjecture was solved*, 1999

"Small factors" at their best: hook length formula

The representation theory of $\mathfrak{S}_n$ and $\mathrm{GL}(N)$, with Young diagrams and (standard and semi-standard) Young tableaux (SYT, SSYT), is the most famous source of enumerations with small factors...

$\lambda = (5,3,3,2)$

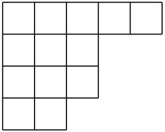

1	2	4	7	13
3	6	10		
5	9	11		
8	12			

1	1	3	4	6
2	3	4		
4	4	5		
6	6			

$N \geq 6$

Q: How many SYT and SSYT for a given diagram λ?

A: Hook formulas, and the Weyl character formula:

Q: Maybe the A_n's are $\#\mathrm{SSYT}(\lambda_n, N)$ for a family of λ_n?

A: YES, for $N = 2n$, $\lambda_n = (n-1, n-1, \dots, 1, 1)$

"Small factors" at their best: hook length formula

The representation theory of $\mathfrak{S}_n$ and $\mathrm{GL}(N)$, with Young diagrams and (standard and semi-standard) Young tableaux (SYT, SSYT), is the most famous source of enumerations with small factors...

$\lambda = (5,3,3,2)$

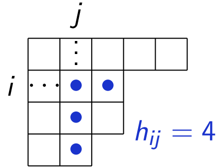

1	2	4	7	13
3	6	10		
5	9	11		
8	12			

1	1	3	4	6
2	3	4		
4	4	5		
6	6			

$N \geq 6$

Q: How many SYT and SSYT for a given diagram λ?
A: Hook formulas, and the Weyl character formula:

$$\#\mathrm{SYT}(\lambda) = \frac{n!}{\prod_{(ij)\in\lambda} h_{ij}}$$

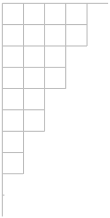

Q: Maybe the A_n's are $\#\mathrm{SSYT}(\lambda_n, N)$ for a family of λ_n?
A: YES, for $N = 2n$, $\lambda_n = (n-1, n-1, \dots, 1, 1)$

"Small factors" at their best: hook length formula

The representation theory of $\mathfrak{S}_n$ and $\mathrm{GL}(N)$, with Young diagrams and (standard and semi-standard) Young tableaux (SYT, SSYT), is the most famous source of enumerations with small factors...

$\lambda = (5,3,3,2)$

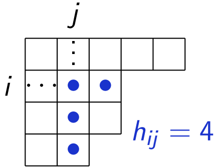

1	2	4	7	13
3	6	10		
5	9	11		
8	12			

1	1	3	4	6
2	3	4		
4	4	5		
6	6			

$N \geq 6$

Q: How many SYT and SSYT for a given diagram λ?

A: Hook formulas, and the Weyl character formula:

$$\#\mathrm{SSYT}(\lambda, N) = \prod_{(ij)\in\lambda} \frac{N+j-i}{h_{ij}} = \prod_{i<j} \frac{(j-\lambda_j)-(i-\lambda_i)}{j-i}$$

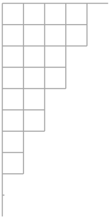

Q: Maybe the A_n's are $\#\mathrm{SSYT}(\lambda_n, N)$ for a family of λ_n?

A: YES, for $N = 2n$, $\lambda_n = (n-1, n-1, \dots, 1, 1)$

"Small factors" at their best: hook length formula

The representation theory of $\mathfrak{S}_n$ and $\mathrm{GL}(N)$, with Young diagrams and (standard and semi-standard) Young tableaux (SYT, SSYT), is the most famous source of enumerations with small factors...

$\lambda = (5, 3, 3, 2)$

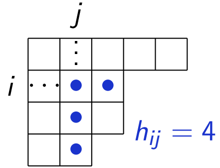

1	2	4	7	13
3	6	10		
5	9	11		
8	12			

1	1	3	4	6
2	3	4		
4	4	5		
6	6			

$N \geq 6$

Q: How many SYT and SSYT for a given diagram λ?
A: Hook formulas, and the Weyl character formula:

$$\#\mathrm{SSYT}(\lambda, N) = \prod_{(ij)\in\lambda} \frac{N + j - i}{h_{ij}} = \prod_{i<j} \frac{(j - \lambda_j) - (i - \lambda_i)}{j - i}$$

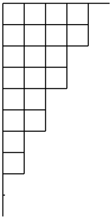

Q: Maybe the A_n's are $\#\mathrm{SSYT}(\lambda_n, N)$ for a family of λ_n?
A: YES, for $N = 2n$, $\lambda_n = (n - 1, n - 1, \ldots, 1, 1)$

Schur polynomials and SSYT's

More precisely, $A_n = 3^{-\binom{n}{2}} \#\mathrm{SSYT}(\lambda_n, 2n)$.

... Now recall that the $\#\mathrm{SSYT}$'s are evaluations at $\mathbf{z} = \mathbf{1}$ of the corresponding Schur polynomials $s_\lambda(z_1, \ldots, z_N)$, $\qquad (\ell(\lambda) \leq N)$

$$s_\lambda(\mathbf{z}) = \frac{\det(z_i^{\lambda_j + N - j})}{\det(z_i^{N-j})} \qquad s_\lambda(\mathbf{1}) = \#\mathrm{SSYT}(\lambda, N)$$

Q: Maybe $s_{\lambda_n}(\mathbf{z})$ gives a weighted enumeration of ASM?
A: YES, this weighted enumeration is the one corresponding to the (physicists') 6 Vertex Model

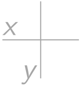

$$q = e^{\frac{2\pi i}{3}} \qquad \underbrace{\tfrac{1}{\sqrt{q}}y - \sqrt{q}x} \qquad \underbrace{\tfrac{1}{\sqrt{q}}x - \sqrt{q}y} \qquad \underbrace{\tfrac{1}{q} - q} \qquad \underbrace{\left(\tfrac{1}{q} - q\right)xy}$$

Schur polynomials and SSYT's

More precisely, $A_n = 3^{-\binom{n}{2}} \#\mathrm{SSYT}(\lambda_n, 2n)$.

…Now recall that the $\#\mathrm{SSYT}$'s are evaluations at $\mathbf{z} = \mathbf{1}$ of the corresponding Schur polynomials $s_\lambda(z_1, \dots, z_N)$, $\qquad (\ell(\lambda) \leq N)$

$$s_\lambda(\mathbf{z}) = \frac{\det(z_i^{\lambda_j + N - j})}{\det(z_i^{N-j})} \qquad s_\lambda(\mathbf{1}) = \#\mathrm{SSYT}(\lambda, N)$$

Q: Maybe $s_{\lambda_n}(\mathbf{z})$ gives a weighted enumeration of ASM?
A: YES, this weighted enumeration is the one corresponding to the (physicists') 6 Vertex Model

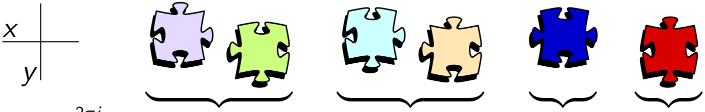

$q = e^{\frac{2\pi i}{3}}$ $\qquad \frac{1}{\sqrt{q}} y - \sqrt{q} x \qquad \frac{1}{\sqrt{q}} x - \sqrt{q} y \qquad \frac{1}{q} - q \qquad \left(\frac{1}{q} - q\right) xy$

Arrows on lines: The 6-Vertex Model

The 6-Vertex Model:

- you have a degree-4 graph $\mathcal{G}$,
- variables are edge-orientations,
- weights are on the vertices,

it is Yang-Baxter–integrable
if weights depend on positions
through spectral parameters
attached to the lines,
and a global parameter q

Arrows on lines: The 6-Vertex Model

The 6-Vertex Model:

- you have a degree-4 graph $\mathcal{G}$,
- variables are edge-orientations,
- weights are on the vertices,

it is Yang-Baxter–integrable
if weights depend on positions
through spectral parameters
attached to the lines,
and a global parameter q

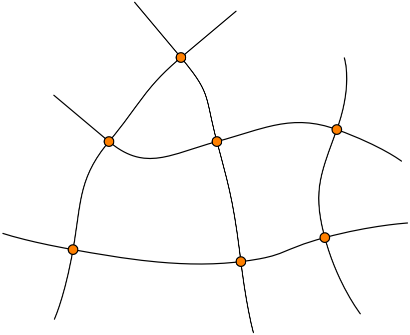

Arrows on lines : The 6-Vertex Model

The 6-Vertex Model:

- you have a degree-4 graph $\mathcal{G}$,
- variables are edge-orientations,
- weights are on the vertices,

it is Yang-Baxter–integrable
if weights depend on positions
through spectral parameters
attached to the lines,
and a global parameter q

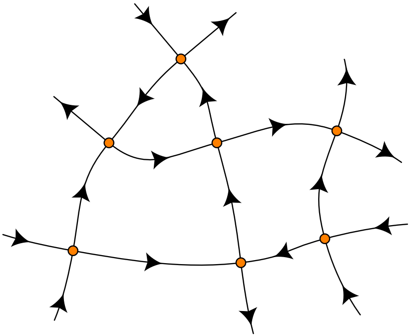

Arrows on lines: The 6-Vertex Model

The 6-Vertex Model:

- you have a degree-4 graph $\mathcal{G}$,
- variables are edge-orientations,
- weights are on the vertices,

it is Yang-Baxter–integrable
if weights depend on positions
through spectral parameters
attached to the lines,
and a global parameter q

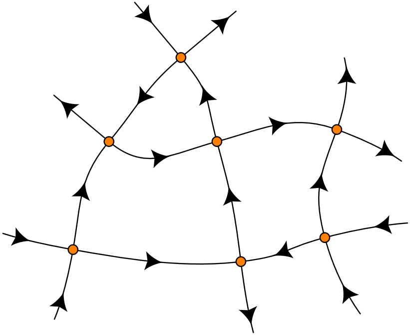

Arrows on lines : The 6-Vertex Model

The 6-Vertex Model:

- you have a degree-4 graph $\mathcal{G}$,
- variables are edge-orientations,
- weights are on the vertices,

it is Yang-Baxter–integrable
if weights depend on positions
through spectral parameters
attached to the lines,
and a global parameter q

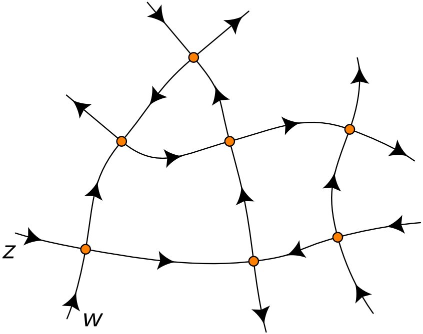

Arrows on lines : The 6-Vertex Model

The 6-Vertex Model:

- you have a degree-4 graph $\mathcal{G}$,
- variables are edge-orientations,
- weights are on the vertices,

it is Yang-Baxter–integrable
if weights depend on positions
through spectral parameters
attached to the lines,
and a global parameter q

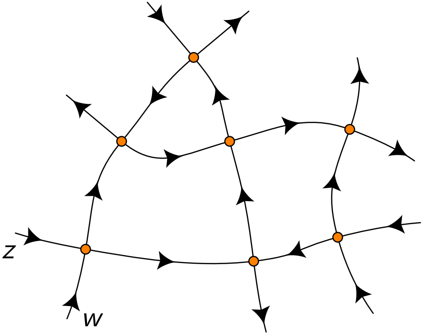

$a = zq - w/q$ $\qquad$ $b = z - w$ $\qquad$ $c = (1/q - q)\sqrt{zw}$

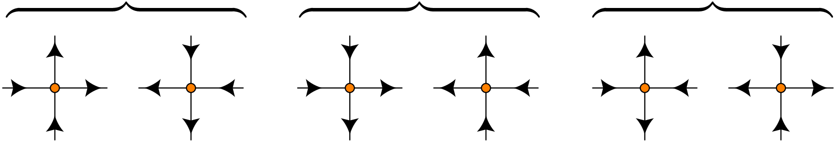

The 6-Vertex Model:

- you have a degree-4 graph $\mathcal{G}$,
- variables are edge-orientations,
- weights are on the vertices,

it is Yang-Baxter–integrable
if weights depend on positions
through spectral parameters
attached to the lines,
and a global parameter q

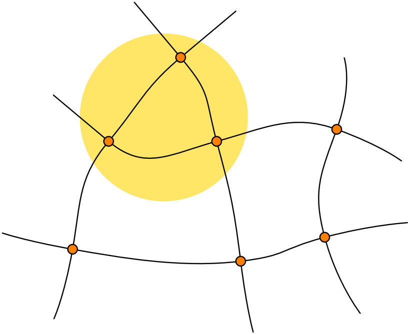

$a = zq - w/q$ $\quad$ $b = z - w$ $\quad$ $c = (1/q - q)\sqrt{zw}$

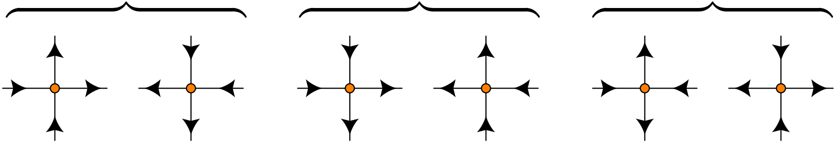

Arrows on lines : The 6-Vertex Model

The 6-Vertex Model:

- you have a degree-4 graph $\mathcal{G}$,
- variables are edge-orientations,
- weights are on the vertices,

it is Yang-Baxter–integrable
if weights depend on positions
through spectral parameters
attached to the lines,
and a global parameter q

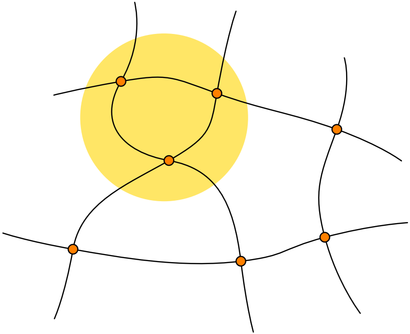

$a = zq - w/q$ $\qquad$ $b = z - w$ $\qquad$ $c = (1/q - q)\sqrt{zw}$

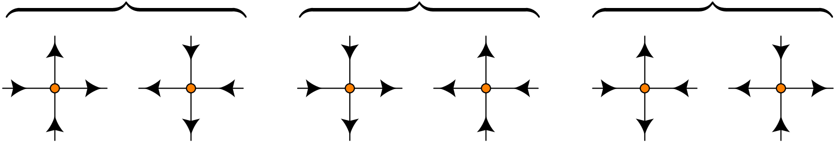

Arrows on lines : The 6-Vertex Model

The 6-Vertex Model:

- you have a degree-4 graph $\mathcal{G}$,
- variables are edge-orientations,
- weights are on the vertices,

it is Yang-Baxter–integrable
if weights depend on positions
through spectral parameters
attached to the lines,
and a global parameter q

$$\Delta = \frac{a^2 + b^2 - c^2}{2ab} = \frac{1}{2}\left(q + \frac{1}{q}\right)$$

$$a = zq - w/q \qquad b = z - w \qquad c = (1/q - q)\sqrt{zw}$$

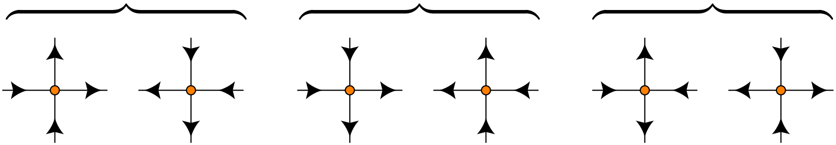

A happy ending. . . and a new beginning

Robbins and Rumsey, 1982	introduce ASM's, and conjecture $A_n = \prod_{j=0}^{n-1} \frac{(3j+1)!}{(n+j)!}$
Andrews, 1994	counts Descending Plane Partitions
Zeilberger, 1994-96	first 'nightmare proof' of A_n formula (using Andrews DPP result)
Kuperberg, 1996	easy proof of A_n formula, using the 6 Vertex Model DWBC gen. function
Okada, 2004	connection with Schur functions and characters of classical groups

Razumov and Stroganov, in 2001, find a (completely different) surprising relation between ASM's and the XXZ Quantum Spin Chain at $\Delta = -\frac{1}{2}$. . .

. . . the Razumov–Stroganov conjecture . . .

A happy ending. . . and a new beginning

Robbins and Rumsey, 1982	introduce ASM's, and conjecture $A_n = \prod_{j=0}^{n-1} \frac{(3j+1)!}{(n+j)!}$
Andrews, 1994	counts Descending Plane Partitions
Zeilberger, 1994-96	first 'nightmare proof' of A_n formula (using Andrews DPP result)
Kuperberg, 1996	easy proof of A_n formula, using the 6 Vertex Model DWBC gen. function
Okada, 2004	connection with Schur functions and characters of classical groups

Razumov and Stroganov, in 2001, find a (completely different) surprising relation between ASM's and the XXZ Quantum Spin Chain at $\Delta = -\frac{1}{2}$. . .

. . . the Razumov–Stroganov conjecture . . .

ASM's and 6-Vertex Model with DWBC

A trivial re-drawing of the tiles relates our 'puzzles' to the 6-Vertex Model on a $n \times n$ square, with "domain-wall boundary conditions".

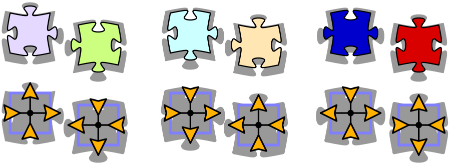

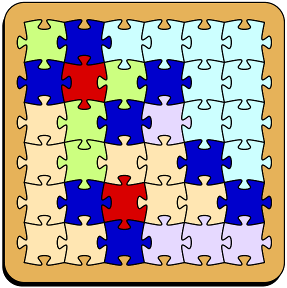

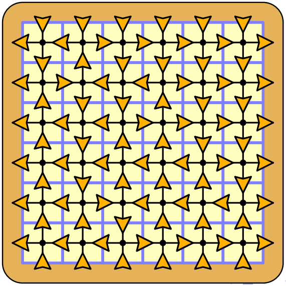

ASM's and Fully Packed Loops

Now consider the following trivial (chessboard) bijection:

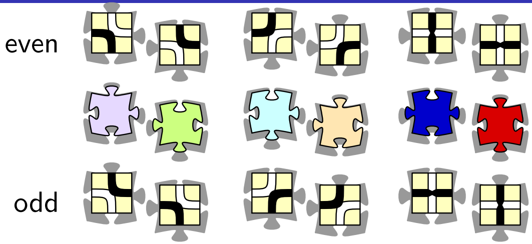

The outcome of a ASM is a Fully Packed Loop configuration (FPL), with alternating boundary conditions

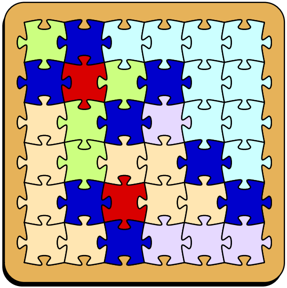

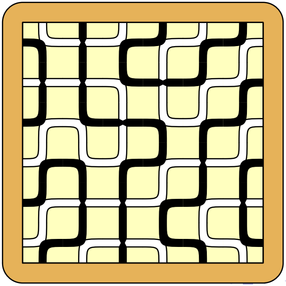

ASM's and Fully Packed Loops

Now consider the following trivial (chessboard) bijection:

even

odd

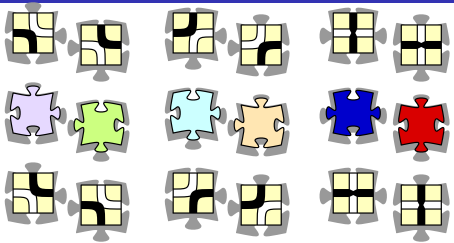

The outcome of a ASM is a Fully Packed Loop configuration (FPL), with alternating boundary conditions

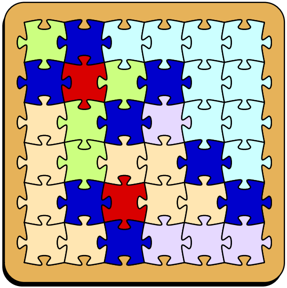

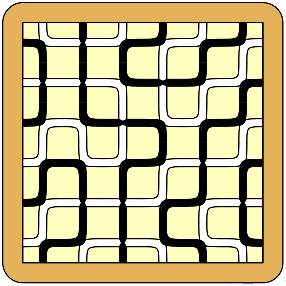

From now on, we will concentrate on this graphical representation.

Link patterns in Fully-Packed Loops

The nice property of Fully-Packed Loop configurations is that they split into rich natural classes, according to their link pattern π for the connectivities among the black terminations on the boundary. (Loops, if present, are just ignored.)

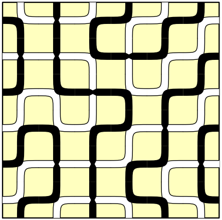

Link patterns in Fully-Packed Loops

The nice property of Fully-Packed Loop configurations is that they split into rich natural classes, according to their link pattern π for the connectivities among the black terminations on the boundary. (Loops, if present, are just ignored.)

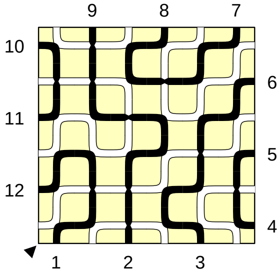

Link patterns in Fully-Packed Loops

The nice property of Fully-Packed Loop configurations is that they split into rich natural classes, according to their link pattern π for the connectivities among the black terminations on the boundary. (Loops, if present, are just ignored.)

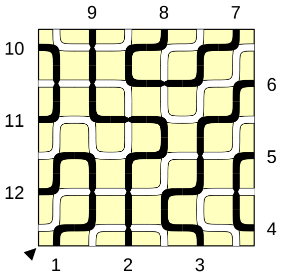

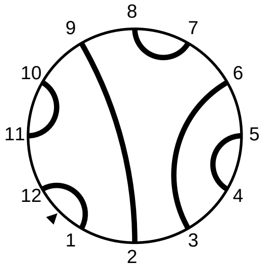

Link patterns in Fully-Packed Loops

The nice property of Fully-Packed Loop configurations is that they split into rich natural classes, according to their link pattern π for the connectivities among the black terminations on the boundary. (Loops, if present, are just ignored.)

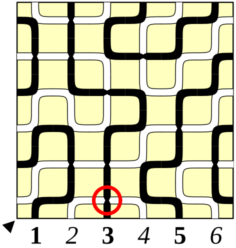

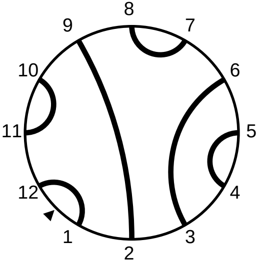

Consider the bottom row. In any FPL configuration, there is a unique straight tile. Call refinement position the corresponding column index.
Refined countings of FPL/ASM's also give “nice” formulas...

$O(1)$ Dense Loop Model / XXZ $\Delta = -\frac{1}{2}$ spin chain

Consider dense loop configurations on a semi-infinite cylinder i.e. tilings of $\{1, \ldots, 2n\} \times \mathbb{N}$ with the two tiles ,  (with the uniform measure)

Link patterns are naturally associated also to these (infinite!) configurations

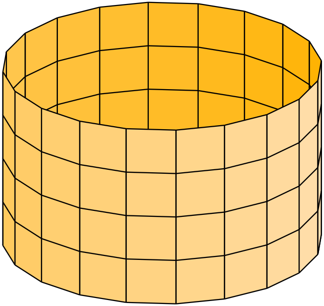

$O(1)$ Dense Loop Model / XXZ $\Delta = -\frac{1}{2}$ spin chain

Consider dense loop configurations on a semi-infinite cylinder i.e. tilings of $\{1, \ldots, 2n\} \times \mathbb{N}$ with the two tiles ,  (with the uniform measure)

Link patterns are naturally associated also to these (infinite!) configurations

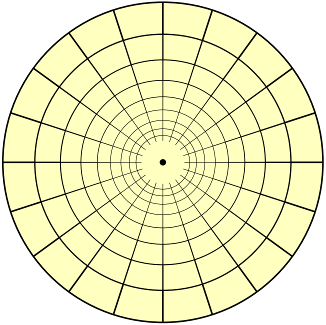

$O(1)$ Dense Loop Model / XXZ $\Delta = -\frac{1}{2}$ spin chain

Consider dense loop configurations on a semi-infinite cylinder i.e. tilings of $\{1, \ldots, 2n\} \times \mathbb{N}$ with the two tiles ,  (with the uniform measure)

Link patterns are naturally associated also to these (infinite!) configurations

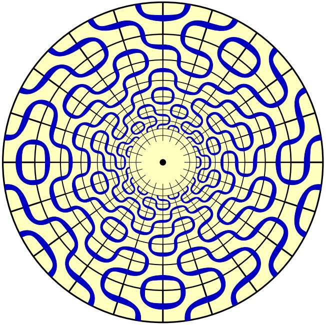

$O(1)$ Dense Loop Model / XXZ $\Delta = -\frac{1}{2}$ spin chain

Consider dense loop configurations on a semi-infinite cylinder i.e. tilings of $\{1, \ldots, 2n\} \times \mathbb{N}$ with the two tiles  , 
(with the uniform measure)

Link patterns are naturally associated also to these (infinite!) configurations

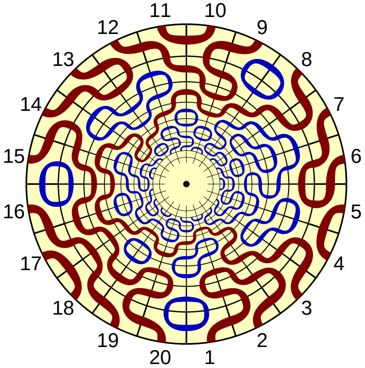

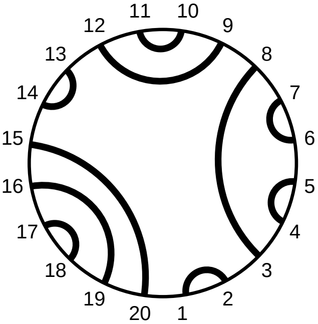

The Razumov–Stroganov correspondence

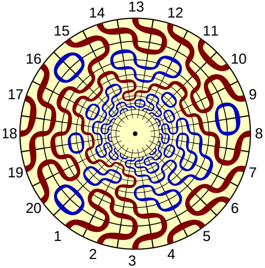

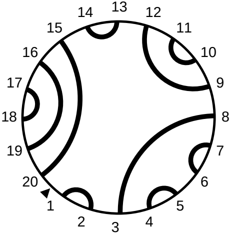

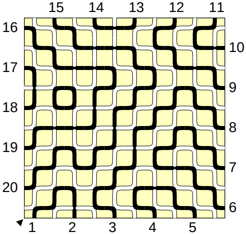

$\tilde{\Psi}_n(\pi)$: probability of π
in the $O(1)$ Dense Loop Model
in the $\{1, \dots, 2n\} \times \mathbb{N}$ cylinder

$\Psi_n(\pi)$: probability of π
for FPL with uniform measure
in the $n \times n$ square

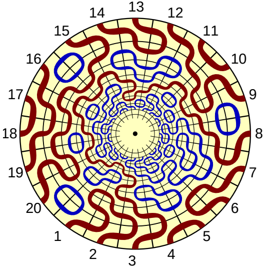

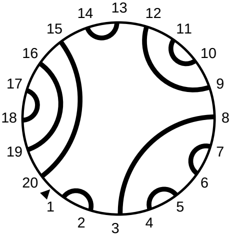

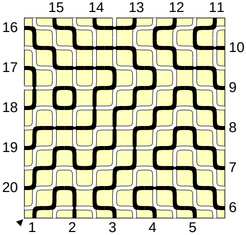

$\tilde{\Psi}_n(\pi)$: probability of π
in the $O(1)$ Dense Loop Model
in the $\{1, \dots, 2n\} \times \mathbb{N}$ cylinder

$\Psi_n(\pi)$: probability of π
for FPL with uniform measure
in the $n \times n$ square

Razumov–Stroganov correspondence
(conjecture: Razumov Stroganov, 2001; proof: AS Cantini, 2010)

$$\tilde{\Psi}_n(\pi) = \Psi_n(\pi)$$

Dihedral symmetry of FPL

A corollary of the Razumov–Stroganov correspondence. . .
(. . . that was known *before* the Razumov–Stroganov conjecture)

call R the operator that rotates a link pattern by one position

Dihedral symmetry of FPL (proof: Wieland, 2000)

$$\Psi_n(\pi) = \Psi_n(R\pi)$$

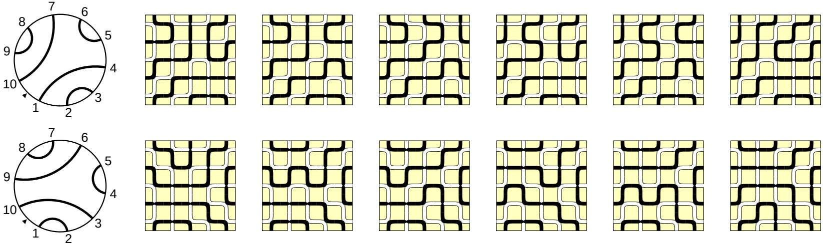

The Temperley-Lieb(1) monoid

Consider the graphical action over link patterns $\pi \in LP(2n)$

(throw away detached cycles)

R :
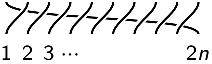

e_j :
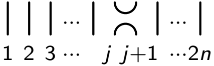

The maps $\{e_j\}_{1 \leq j \leq 2n}$ and $R^{\pm 1}$ generate a semigroup

Example:

$e_1(\pi)$:
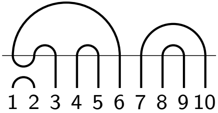

=
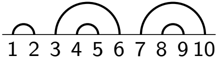

$e_2(\pi)$:
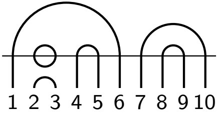

=
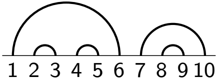

Consider the linear space $\mathbb{C}^{LP(2n)}$, linear span of basis vectors $|\pi\rangle$.
Operators e_j and $R^{\pm 1}$ are linear operators over $\mathbb{C}^{LP(2n)}$

$O(1)$ dense loop model: the Markov Chain over $LP(2n)$

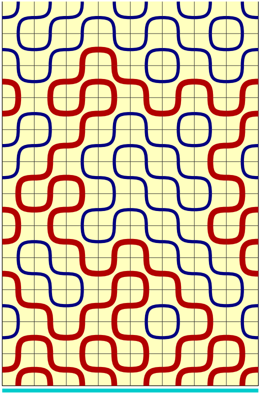

A config with $t-1$ layers.

$O(1)$ dense loop model: the Markov Chain over $LP(2n)$

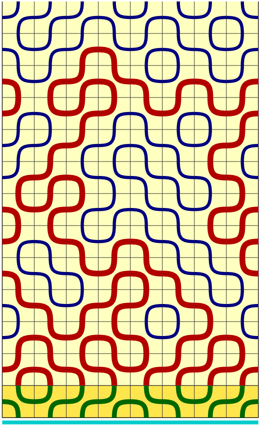

A config with $t-1$ layers.

Add a new layer, of i.i.d. tiles, with prob. p (say, $p=1/2$)...

$O(1)$ dense loop model: the Markov Chain over $LP(2n)$

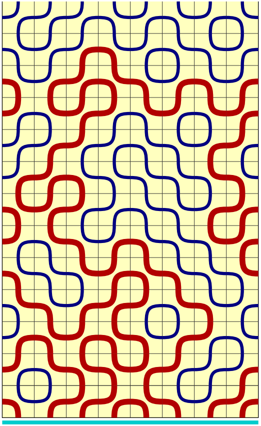

A config with $t - 1$ layers.

Add a new layer, of i.i.d. tiles, with prob. p (say, $p = 1/2$)...

Some loops get detached from the boundary. You have a config with t layers, and a new link pattern.

Rates $T_{p=1/2}(\pi, \pi')$

$O(1)$ dense loop model: the Markov Chain over $LP(2n)$

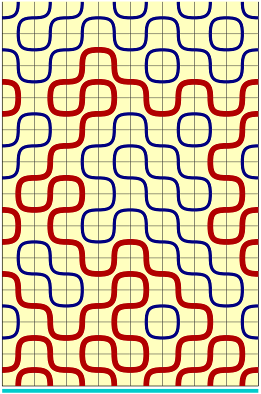

Now repeat the game...

$O(1)$ dense loop model: the Markov Chain over $LP(2n)$

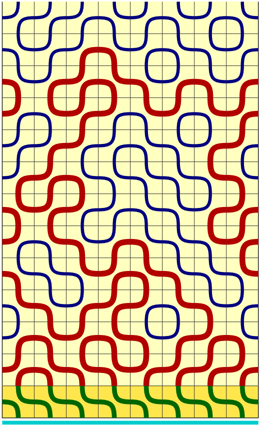

Now repeat the game...

...but add i.i.d. tiles, with prob. $p \to 0$ ...

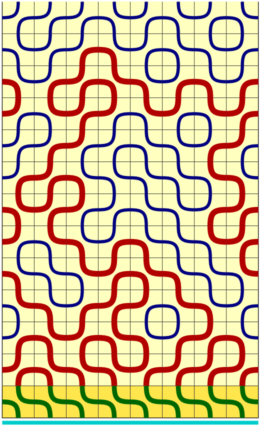

Now repeat the game...

...but add i.i.d. tiles, with prob. $p \to 0$ ...

For most of the layers you just rotate...

$O(1)$ dense loop model: the Markov Chain over $LP(2n)$

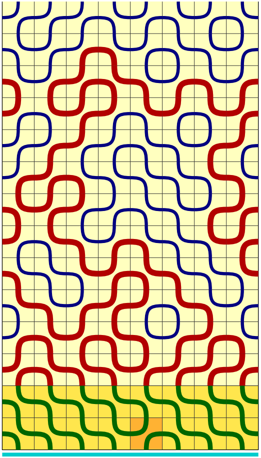

Now repeat the game...

...but add i.i.d. tiles, with prob. $p \to 0$ ...

For most of the layers you just rotate... From time to time, you have a single non-trivial tile.

Rates $T_{p \to 0}(\pi, \pi')$

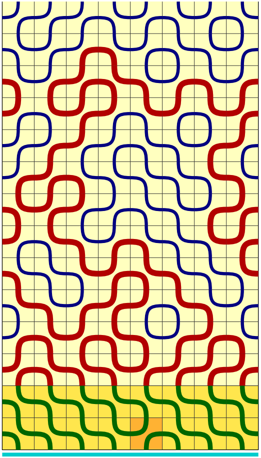

Now repeat the game...

...but add i.i.d. tiles, with prob. $p \to 0$ ...

For most of the layers you just rotate... From time to time, you have a single non-trivial tile.

Rates $T_{p \to 0}(\pi, \pi')$

Non-trivial layers look like operators $R\, e_j$

$$T_p = R\big(I + p \sum_j (e_j - 1) + \mathcal{O}(p^2)\big)$$

$O(1)$ dense loop model: the Markov Chain over $LP(2n)$

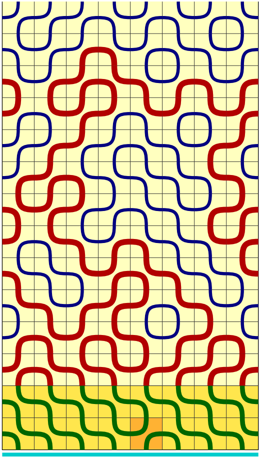

Now repeat the game...

...but add i.i.d. tiles, with prob. $p \to 0$ ...

For most of the layers you just rotate... From time to time, you have a single non-trivial tile.

Rates $T_{p\to 0}(\pi, \pi')$

Non-trivial layers look like operators $R\, e_j$

$$T_p = R\big(I + p \textstyle\sum_j (e_j - 1) + \mathcal{O}(p^2)\big)$$

Hamiltonian H

Integrability: commutation of Transfer Matrices

Call $T_p(\pi, \pi')$ the matrix of transition rates, acting on $\mathbb{C}^{LP(2n)}$ for tiling one layer, with probability p.

Trivial: $\tilde{\Psi}_p(\pi)$, the steady state, is the unique eigenstate of $T_p(\pi, \pi')$ with all positive entries

The Yang–Baxter relation implies: $[T_p, T_{p'}] = 0$

Consequence: $\tilde{\Psi}_p(\pi) \equiv \tilde{\Psi}_{p'}(\pi)$ and we can get $\tilde{\Psi}(\pi) := \tilde{\Psi}_{1/2}(\pi)$ from the study of the easier $T_{p \to 0}(\pi, \pi')$

Call $H_n = \sum_{i=1}^{2n} (e_i - 1)$ and $|\tilde{\Psi}_n\rangle = \sum_\pi \tilde{\Psi}(\pi) |\pi\rangle$

As $R^{-1} T_p = I + pH + \mathcal{O}(p^2)$ we have

$$H_n |\tilde{\Psi}_n\rangle = 0$$

linear-algebra characterization of $\tilde{\Psi}(\pi)$

Integrability: commutation of Transfer Matrices

...said with a picture...

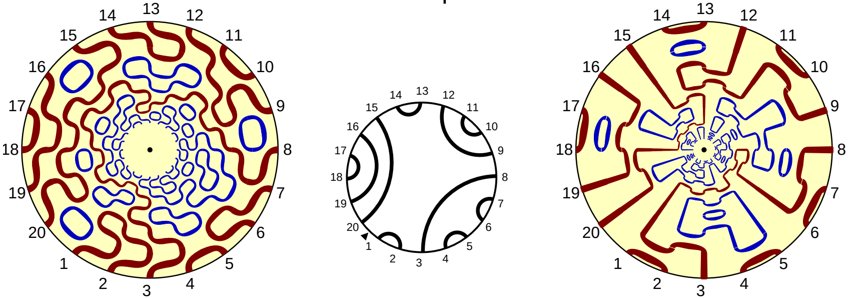

$$|\tilde{\Psi}_n\rangle := \sum_{\pi \in LP(2n)} \tilde{\Psi}_n(\pi)|\pi\rangle \qquad |\tilde{\Psi}_n\rangle := \sum_{\pi \in LP(2n)} \tilde{\Psi}_n(\pi)|\pi\rangle$$

$$(T_n - 1)|\tilde{\Psi}_n\rangle = 0 \qquad H_n|\tilde{\Psi}_n\rangle = 0$$

the two linear equations for $|\tilde{\Psi}_n\rangle$ are equivalent!

The Razumov–Stroganov correspondence: reloaded

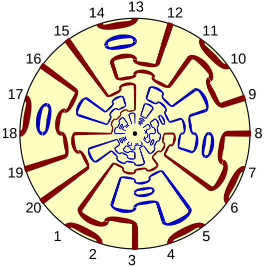

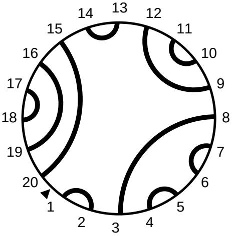

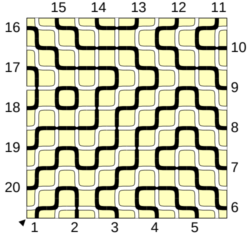

$$|\tilde{\Psi}_n\rangle := \sum_{\pi \in LP(2n)} \tilde{\Psi}_n(\pi)|\pi\rangle$$

$$H_n|\tilde{\Psi}_n\rangle = 0$$

$$|\Psi_n\rangle = \sum_{\phi \in Fpl(n)} |\pi(\phi)\rangle$$

$$Fpl(n) = \{ \text{FPL in } n \times n \text{ square} \}$$

The Razumov–Stroganov correspondence: reloaded

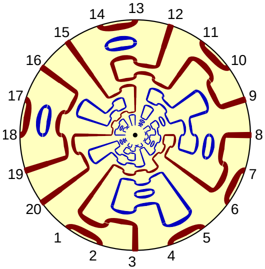

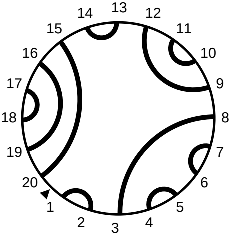

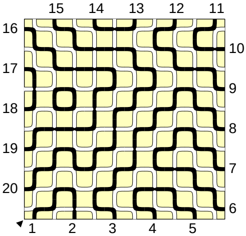

$$|\tilde{\Psi}_n\rangle := \sum_{\pi \in LP(2n)} \tilde{\Psi}_n(\pi)|\pi\rangle$$

$$H_n|\tilde{\Psi}_n\rangle = 0$$

$$|\Psi_n\rangle = \sum_{\phi \in Fpl(n)} |\pi(\phi)\rangle$$

$$Fpl(n) = \{\, \text{FPL in } n \times n \text{ square} \,\}$$

Razumov–Stroganov correspondence
(conjecture: Razumov Stroganov, 2001; proof: AS Cantini, 2010)

$$H_n|\Psi_n\rangle = 0$$

$O(1)$ dense loop model: the Scattering Matrices

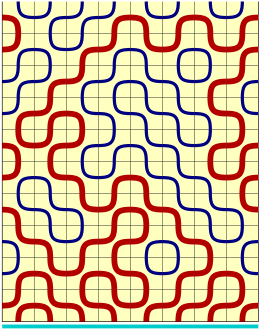

Repeat the game once more...

$O(1)$ dense loop model: the Scattering Matrices

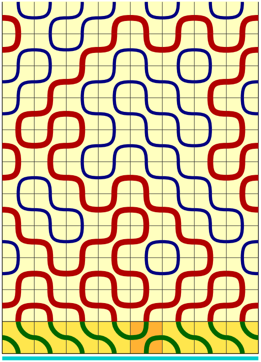

Repeat the game once more...

...but this time keep all tiles frozen, except for the one in column $i+1$

$$RX_i(t) = R(t + (1-t)e_i)$$

...ok, these operators by themselves are not specially nice, nonetheless...

$O(1)$ dense loop model: the Scattering Matrices

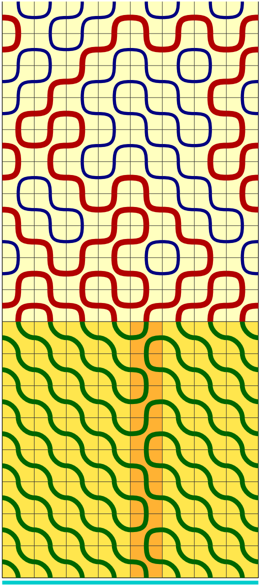

Repeat the game once more...

...but this time keep all tiles frozen, except for the one in column $i + 1$

$$RX_i(t) = R(t + (1 - t)e_i)$$

...ok, these operators by themselves are not specially nice, nonetheless...

...call $S_i(t) = (RX_i(t))^N$ the Scattering Matrix on column i.

$O(1)$ dense loop model: the Scattering Matrices

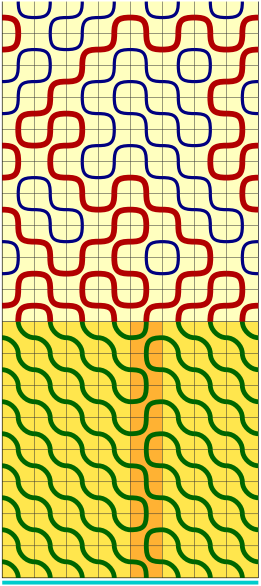

Repeat the game once more...

...but this time keep all tiles frozen, except for the one in column $i+1$

$$RX_i(t) = R(t + (1-t)e_i)$$

...ok, these operators by themselves are not specially nice, nonetheless...

...call $S_i(t) = (RX_i(t))^N$
the Scattering Matrix on column i.

$[S_i(t), S_i(t')]$ is ugly

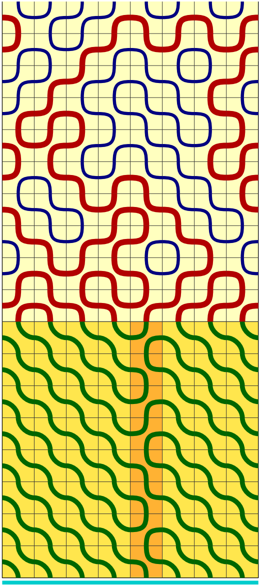

Repeat the game once more...

...but this time keep all tiles frozen, except for the one in column $i+1$

$$RX_i(t) = R(t + (1-t)e_i)$$

...ok, these operators by themselves are not specially nice, nonetheless...

...call $S_i(t) = (RX_i(t))^N$
the Scattering Matrix on column i.

$[S_i(t), S_j(t)]$ is ugly

$O(1)$ dense loop model: the Scattering Matrices

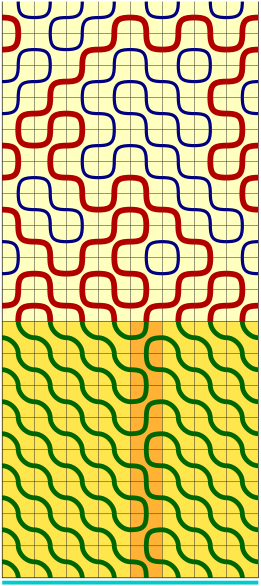

Repeat the game once more...

...but this time keep all tiles frozen, except for the one in column $i+1$

$$RX_i(t) = R(t + (1-t)e_i)$$

...ok, these operators by themselves are not specially nice, nonetheless...

...call $S_i(t) = (RX_i(t))^N$
the Scattering Matrix on column i.

$[S_i(t), T(p)]$ is ugly

$O(1)$ dense loop model: the Scattering Matrices

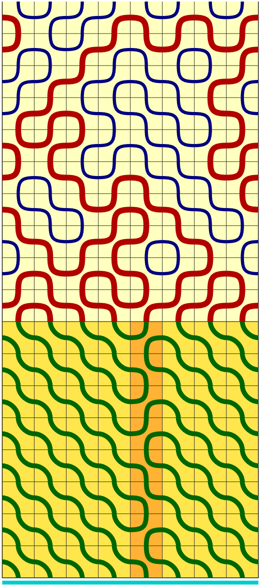

Repeat the game once more...

...but this time keep all tiles frozen, except for the one in column $i+1$

$$RX_i(t) = R(t + (1-t)e_i)$$

...ok, these operators by themselves are not specially nice, nonetheless...

...call $S_i(t) = (RX_i(t))^N$
the Scattering Matrix on column i.

$[S_i(t), H]$ is ugly...

$O(1)$ dense loop model: the Scattering Matrices

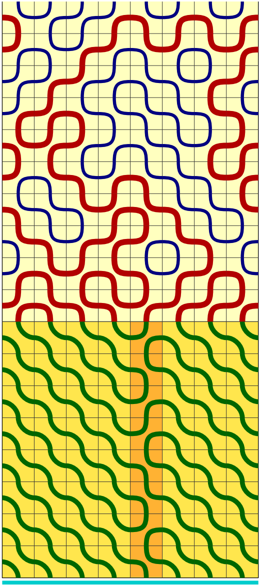

Repeat the game once more...

...but this time keep all tiles frozen, except for the one in column $i+1$

$$RX_i(t) = R(t + (1-t)e_i)$$

...ok, these operators by themselves are not specially nice, nonetheless...

...call $S_i(t) = (RX_i(t))^N$
the Scattering Matrix on column i.

...but $S_i(1-t) = \mathbf{1} + t\,H + \mathcal{O}(t^2)$

$O(1)$ dense loop model: the Scattering Matrices

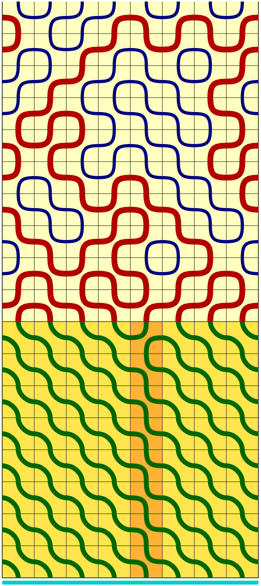

Repeat the game once more...

...but this time keep all tiles frozen, except for the one in column $i+1$

$$RX_i(t) = R(t + (1-t)e_i)$$

...ok, these operators by themselves are not specially nice, nonetheless...

...call $S_i(t) = (RX_i(t))^N$
the Scattering Matrix on column i.

...but $S_i(1-t) = \mathbf{1} + t\,H + \mathcal{O}(t^2)$

$O(1)$ dense loop model: the Scattering Matrices

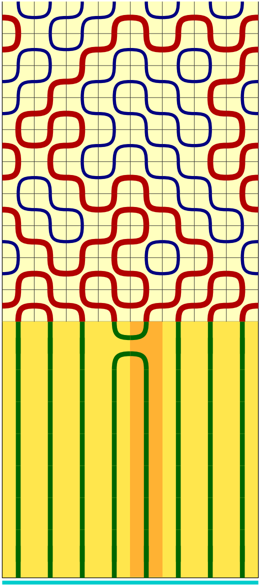

Repeat the game once more...

...but this time keep all tiles frozen, except for the one in column $i+1$

$$RX_i(t) = R(t + (1-t)e_i)$$

...ok, these operators by themselves are not specially nice, nonetheless...

...call $S_i(t) = (RX_i(t))^N$
the Scattering Matrix on column i.

...but $S_i(1-t) = \mathbf{1} + t\,H + \mathcal{O}(t^2)$

$O(1)$ dense loop model: the Scattering Matrices

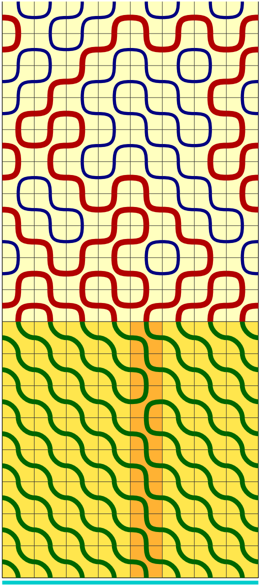

Repeat the game once more...

...but this time keep all tiles frozen, except for the one in column $i+1$

$$RX_i(t) = R(t + (1-t)e_i)$$

...ok, these operators by themselves are not specially nice, nonetheless...

...call $S_i(t) = (RX_i(t))^N$
the Scattering Matrix on column i.

...but $S_i(1-t) = \mathbf{1} + t\,H + \mathcal{O}(t^2)$

$O(1)$ dense loop model: the Scattering Matrices

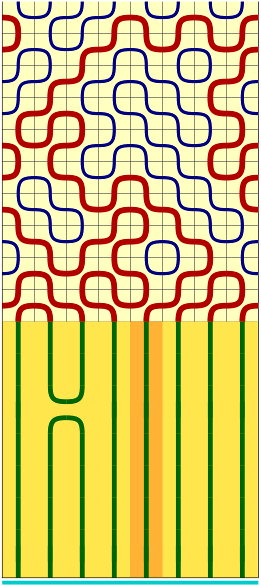

Repeat the game once more...

...but this time keep all tiles frozen, except for the one in column $i+1$

$$RX_i(t) = R(t + (1-t)e_i)$$

...ok, these operators by themselves are not specially nice, nonetheless...

...call $S_i(t) = (RX_i(t))^N$
the Scattering Matrix on column i.

...but $S_i(1-t) = \mathbf{1} + t\,H + \mathcal{O}(t^2)$

$O(1)$ dense loop model: the Scattering Matrices

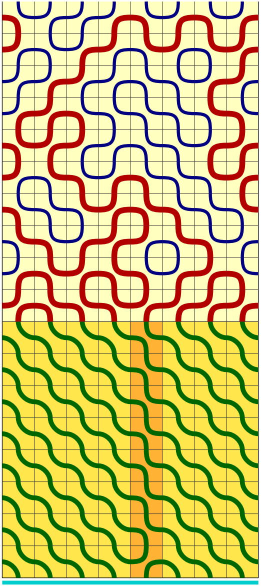

Repeat the game once more...

...but this time keep all tiles frozen, except for the one in column $i+1$

$$RX_i(t) = R(t + (1-t)e_i)$$

...ok, these operators by themselves are not specially nice, nonetheless...

...call $S_i(t) = (RX_i(t))^N$ the Scattering Matrix on column i.

...but $S_i(1-t) = \mathbf{1} + t\,H + \mathcal{O}(t^2)$

$O(1)$ dense loop model: the Scattering Matrices

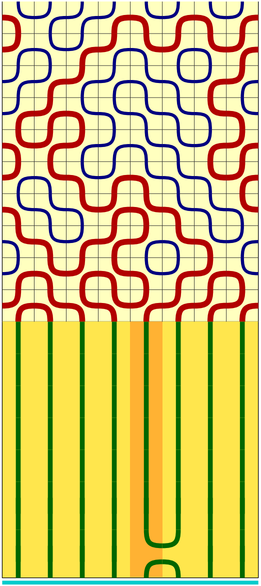

Repeat the game once more...

...but this time keep all tiles frozen, except for the one in column $i+1$

$$RX_i(t) = R(t + (1-t)e_i)$$

...ok, these operators by themselves are not specially nice, nonetheless...

...call $S_i(t) = (RX_i(t))^N$
the Scattering Matrix on column i.

...but $S_i(1-t) = \mathbf{1} + t\ H + \mathcal{O}(t^2)$

$O(1)$ dense loop model: spectral parameters

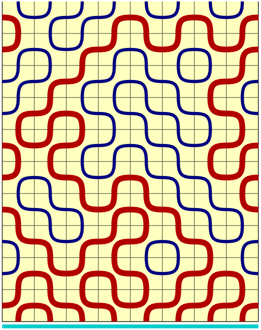

Why the Scattering Matrix has these properties? Why it has a chance of being interesting?. . .

$O(1)$ dense loop model: spectral parameters

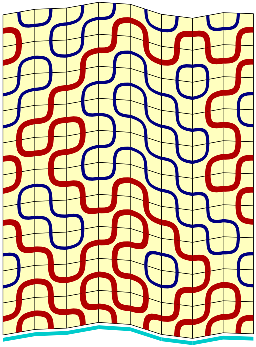

Just like the 6-Vertex Model, also the $O(1)$ Dense Loop Model is Yang-Baxter–integrable, and exists in a version with generic spectral parameters on the lines.

A special choice of vertical parameters leads to $S_i(t)$.

Just like in the 'historical' solution of the 6VM, also here the model with generic parameters is richer, and exchange relations lead to remarkable multi-contour integral formulae.

$O(1)$ dense loop model: spectral parameters

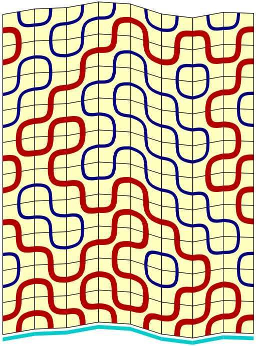

✍ Ph. Di Francesco and P. Zinn-Justin, *Around the Razumov-Stroganov conjecture: proof of a multi-parameter sum rule,* EJC 2005.

✍ Ph. Di Francesco, P. Zinn-Justin and J.-B. Zuber, *Sum Rules for the Ground States of the $O(1)$ Loop Model on a Cylinder and the XXZ Spin Chain,* J. Stat. Mech., 2006.

Dihedral covariance of the ground states

We had $|\tilde{\Psi}_n\rangle = \sum_\pi \tilde{\Psi}(\pi)|\pi\rangle$, satisfying $H_n|\tilde{\Psi}_n\rangle = 0$

The operators $RX_i(t)$, and the scattering matrices $S_i(t)$, induce the deformation
$|\tilde{\Psi}_n^{(i)}(t)\rangle = \sum_\pi \tilde{\Psi}^{(i)}(t;\pi)|\pi\rangle$, satisfying $(RX_i(t) - 1)|\tilde{\Psi}_n^{(i)}(t)\rangle = 0$.

Because of a dihedral covariance of these equations, (and unicity of the Frobenius vector) it suffices to study $RX_1(t)$ and $|\tilde{\Psi}_n^{(1)}(t)\rangle$

Example:

$0 = (X_i(t) - R^{-1})|\tilde{\Psi}_n^{(i)}(t)\rangle = R(X_{i+1}(t) - R^{-1})R^{-1}|\tilde{\Psi}_n^{(i)}(t)\rangle$
implying $|\tilde{\Psi}_n^{(i+1)}(t)\rangle \propto R^{-1}|\tilde{\Psi}_n^{(i)}(t)\rangle$

Call $\mathrm{Sym} = N^{-1}\sum_{i=0}^{N-1} R^i$, the operator that projects on the rotationally-invariant subspace of $\mathbb{C}^{LP(N)}$.

Dihedral covariance of the ground states

We had $|\tilde{\Psi}_n\rangle = \sum_\pi \tilde{\Psi}(\pi)|\pi\rangle$, satisfying $H_n|\tilde{\Psi}_n\rangle = 0$

The operators $RX_i(t)$, and the scattering matrices $S_i(t)$, induce the deformation

$|\tilde{\Psi}_n^{(i)}(t)\rangle = \sum_\pi \tilde{\Psi}^{(i)}(t;\pi)|\pi\rangle$, satisfying $(RX_i(t) - 1)|\tilde{\Psi}_n^{(i)}(t)\rangle = 0$.

Because of a dihedral covariance of these equations, (and unicity of the Frobenius vector) it suffices to study $RX_1(t)$ and $|\tilde{\Psi}_n^{(1)}(t)\rangle$

Example:

$$0 = (X_i(t) - R^{-1})|\tilde{\Psi}_n^{(i)}(t)\rangle = R(X_{i+1}(t) - R^{-1})R^{-1}|\tilde{\Psi}_n^{(i)}(t)\rangle$$

implying $|\tilde{\Psi}_n^{(i+1)}(t)\rangle \propto R^{-1}|\tilde{\Psi}_n^{(i)}(t)\rangle$

Call $\mathrm{Sym} = N^{-1}\sum_{i=0}^{N-1} R^i$, the operator that projects on the rotationally-invariant subspace of $\mathbb{C}^{LP(N)}$.

Dihedral covariance of the ground states

We had $|\tilde{\Psi}_n\rangle = \sum_\pi \tilde{\Psi}(\pi)|\pi\rangle$, satisfying $H_n|\tilde{\Psi}_n\rangle = 0$

The operators $RX_i(t)$, and the scattering matrices $S_i(t)$, induce the deformation
$|\tilde{\Psi}_n^{(i)}(t)\rangle = \sum_\pi \tilde{\Psi}^{(i)}(t;\pi)|\pi\rangle$, satisfying $(RX_i(t) - 1)|\tilde{\Psi}_n^{(i)}(t)\rangle = 0$.

Because of a dihedral covariance of these equations,
(and unicity of the Frobenius vector)
it suffices to study $RX_1(t)$ and $|\tilde{\Psi}_n^{(1)}(t)\rangle$

Example:

$$0 = (X_i(t) - R^{-1})|\tilde{\Psi}_n^{(i)}(t)\rangle = R(X_{i+1}(t) - R^{-1})R^{-1}|\tilde{\Psi}_n^{(i)}(t)\rangle$$

implying $|\tilde{\Psi}_n^{(i+1)}(t)\rangle \propto R^{-1}|\tilde{\Psi}_n^{(i)}(t)\rangle$

Call $\mathrm{Sym} = N^{-1}\sum_{i=0}^{N-1} R^i$, the operator that projects on the rotationally-invariant subspace of $\mathbb{C}^{LP(N)}$.

Dihedral covariance of the ground states

We had $|\tilde{\Psi}_n\rangle = \sum_\pi \tilde{\Psi}(\pi)|\pi\rangle$, satisfying $H_n|\tilde{\Psi}_n\rangle = 0$

The operators $RX_i(t)$, and the scattering matrices $S_i(t)$, induce the deformation
$|\tilde{\Psi}_n^{(i)}(t)\rangle = \sum_\pi \tilde{\Psi}^{(i)}(t;\pi)|\pi\rangle$, satisfying $(RX_i(t) - 1)|\tilde{\Psi}_n^{(i)}(t)\rangle = 0$.

Because of a dihedral covariance of these equations,
(and unicity of the Frobenius vector)
it suffices to study $RX_1(t)$ and $|\tilde{\Psi}_n^{(1)}(t)\rangle$

Example:

$$0 = (X_i(t) - R^{-1})|\tilde{\Psi}_n^{(i)}(t)\rangle = R(X_{i+1}(t) - R^{-1})R^{-1}|\tilde{\Psi}_n^{(i)}(t)\rangle$$

implying $|\tilde{\Psi}_n^{(i+1)}(t)\rangle \propto R^{-1}|\tilde{\Psi}_n^{(i)}(t)\rangle$

Call $\mathrm{Sym} = N^{-1}\sum_{i=0}^{N-1} R^i$, the operator that projects on the rotationally-invariant subspace of $\mathbb{C}^{LP(N)}$.

Dihedral covariance of the ground states

We had $|\tilde{\Psi}_n\rangle = \sum_\pi \tilde{\Psi}(\pi)|\pi\rangle$, satisfying $H_n|\tilde{\Psi}_n\rangle = 0$

The operators $RX_i(t)$, and the scattering matrices $S_i(t)$,
induce the deformation
$|\tilde{\Psi}_n^{(i)}(t)\rangle = \sum_\pi \tilde{\Psi}^{(i)}(t;\pi)|\pi\rangle$, satisfying $(RX_i(t) - 1)|\tilde{\Psi}_n^{(i)}(t)\rangle = 0$.

Because of a dihedral covariance of these equations,
(and unicity of the Frobenius vector)
it suffices to study $RX_1(t)$ and $|\tilde{\Psi}_n^{(1)}(t)\rangle$

Example:

$$0 = (X_i(t) - R^{-1})|\tilde{\Psi}_n^{(i)}(t)\rangle = R(X_{i+1}(t) - R^{-1})R^{-1}|\tilde{\Psi}_n^{(i)}(t)\rangle$$

implying $|\tilde{\Psi}_n^{(i+1)}(t)\rangle \propto R^{-1}|\tilde{\Psi}_n^{(i)}(t)\rangle$

Call $\mathrm{Sym} = N^{-1}\sum_{i=0}^{N-1} R^i$, the operator that projects on the rotationally-invariant subspace of $\mathbb{C}^{LP(N)}$.

The refined Razumov–Stroganov correspondence

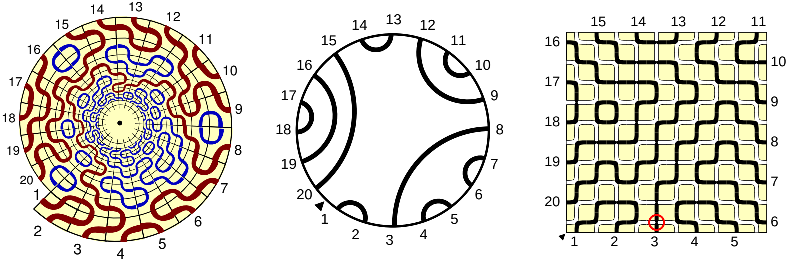

$\tilde{\Psi}_n(t;\pi)$: probability of π in the $O(1)$ Dense Loop Model with dynamics given by $RX_1(t)$

$\Psi_n(t;\pi)$: count FPL's ϕ having link pattern π give $t^{h(\phi)-1}$ weight

The refined Razumov–Stroganov correspondence

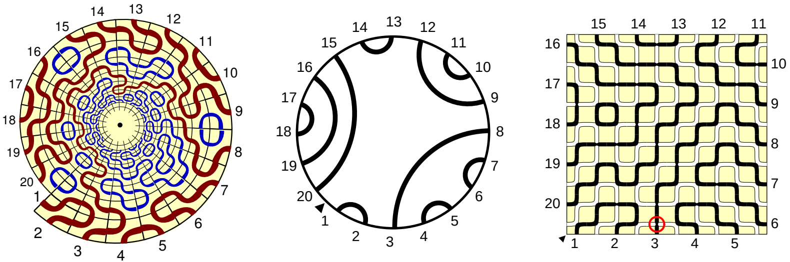

$\tilde{\Psi}_n(t;\pi)$: probability of π in the $O(1)$ Dense Loop Model with dynamics given by $RX_1(t)$

$\Psi_n(t;\pi)$: count FPL's ϕ having link pattern π give $t^{h(\phi)-1}$ weight

Refined Razumov–Stroganov correspondence
(conjecture: Di Francesco, 2004; proof: AS Cantini, 2012)

$$\tilde{\Psi}_n(t;\pi) \neq \Psi_n(t;\pi)$$

The refined Razumov–Stroganov correspondence

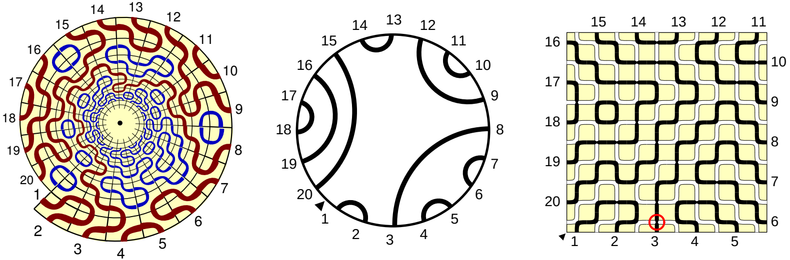

$\tilde{\Psi}_n(t;\pi)$: probability of π
in the $O(1)$ Dense Loop Model
with dynamics given by $RX_1(t)$

$\Psi_n(t;\pi)$: count FPL's ϕ
having link pattern π
give $t^{h(\phi)-1}$ weight

Refined Razumov–Stroganov correspondence
(conjecture: Di Francesco, 2004; proof: AS Cantini, 2012)

$$|\tilde{\Psi}_n(t)\rangle \neq |\Psi_n(t)\rangle$$

The refined Razumov–Stroganov correspondence

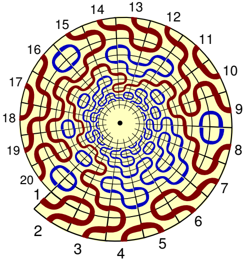

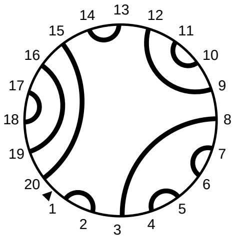

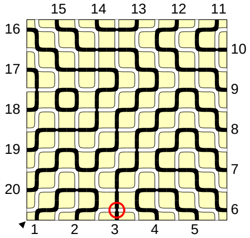

$\tilde{\Psi}_n(t;\pi)$: probability of π in the $O(1)$ Dense Loop Model with dynamics given by $RX_1(t)$

$\Psi_n(t;\pi)$: count FPL's ϕ having link pattern π give $t^{h(\phi)-1}$ weight

Refined Razumov–Stroganov correspondence

(conjecture: Di Francesco, 2004; proof: AS Cantini, 2012)

$$\mathrm{Sym}\,|\tilde{\Psi}_n(t)\rangle = \mathrm{Sym}\,|\Psi_n(t)\rangle$$

A quest for a new strategy

The strategy in the 2010 RS proof, by L. Cantini and me, was

- Realize that $H|\tilde{\Psi}\rangle = 0$ fixes $|\tilde{\Psi}\rangle$ univocally;
- Prove combinatorially that also $|\Psi\rangle$ satisfies $H|\Psi\rangle = 0$...

...But the $|\tilde{\Psi}^{(i)}\rangle$'s differ (they are only dihedrally covariant), and satisfy different linear equations (with $RX_i(t)$)...

...and $\mathrm{Sym}\,|\tilde{\Psi}^{(i)}\rangle$ does not satisfy any simple linear equation that fixes it univocally!

Best possible hope:

- Find a new way $\pi'(\phi)$ of associating link patterns to FPL;
- Find&prove $|\tilde{\Psi}(t)\rangle = |\Psi'(t)\rangle$ with no need of symmetrization;
- Prove combinatorially that $\mathrm{Sym}\,|\Psi'(t)\rangle = \mathrm{Sym}\,|\Psi(t)\rangle$

Bonus: The new enumeration is interesting by itself

A quest for a new strategy

The strategy in the 2010 RS proof, by L. Cantini and me, was

- Realize that $H|\tilde{\Psi}\rangle = 0$ fixes $|\tilde{\Psi}\rangle$ univocally;
- Prove combinatorially that also $|\Psi\rangle$ satisfies $H|\Psi\rangle = 0$...

...But the $|\tilde{\Psi}^{(i)}\rangle$'s differ (they are only dihedrally covariant), and satisfy different linear equations (with $RX_i(t)$)...

...and $\mathrm{Sym}\ |\tilde{\Psi}^{(i)}\rangle$ does not satisfy any simple linear equation that fixes it univocally!

Best possible hope:

- Find a new way $\pi'(\phi)$ of associating link patterns to FPL;
- Find&prove $|\tilde{\Psi}(t)\rangle = |\Psi'(t)\rangle$ with no need of symmetrization;
- Prove combinatorially that $\mathrm{Sym}\ |\Psi'(t)\rangle = \mathrm{Sym}\ |\Psi(t)\rangle$

Bonus: The new enumeration is interesting by itself

A quest for a new strategy

The strategy in the 2010 RS proof, by L. Cantini and me, was

- Realize that $H|\tilde{\Psi}\rangle = 0$ fixes $|\tilde{\Psi}\rangle$ univocally;
- Prove combinatorially that also $|\Psi\rangle$ satisfies $H|\Psi\rangle = 0$...

...But the $|\tilde{\Psi}^{(i)}\rangle$'s differ (they are only dihedrally covariant), and satisfy different linear equations (with $RX_i(t)$)...

...and $\mathrm{Sym}\,|\tilde{\Psi}^{(i)}\rangle$ does not satisfy any simple linear equation that fixes it univocally!

Best possible hope:

- Find a new way $\pi'(\phi)$ of associating link patterns to FPL;
- Find&prove $|\tilde{\Psi}(t)\rangle = |\Psi'(t)\rangle$ with no need of symmetrization;
- Prove combinatorially that $\mathrm{Sym}\,|\Psi'(t)\rangle = \mathrm{Sym}\,|\Psi(t)\rangle$

Bonus: The new enumeration is interesting by itself

A quest for a new strategy

The strategy in the 2010 RS proof, by L. Cantini and me, was

- Realize that $H|\tilde{\Psi}\rangle = 0$ fixes $|\tilde{\Psi}\rangle$ univocally;
- Prove combinatorially that also $|\Psi\rangle$ satisfies $H|\Psi\rangle = 0$...

...But the $|\tilde{\Psi}^{(i)}\rangle$'s differ (they are only dihedrally covariant), and satisfy different linear equations (with $RX_i(t)$)...

...and $\mathrm{Sym}\,|\tilde{\Psi}^{(i)}\rangle$ does not satisfy any simple linear equation that fixes it univocally!

Best possible hope:

- Find a new way $\pi'(\phi)$ of associating link patterns to FPL;
- Find&prove $|\tilde{\Psi}(t)\rangle = |\Psi'(t)\rangle$ with no need of symmetrization;
- Prove combinatorially that $\mathrm{Sym}\,|\Psi'(t)\rangle = \mathrm{Sym}\,|\Psi(t)\rangle$

Bonus: The new enumeration is interesting by itself

The heretical enumeration

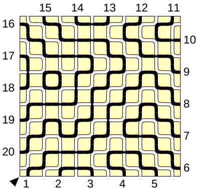

The role of black and white is symmetrical...

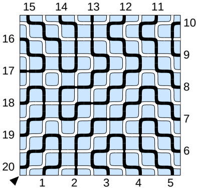

...who's who is a matter of convention.

Swapping coloration in all FPL's leads to an equivalent conjecture

The heretical enumeration

$\pi(\phi)$

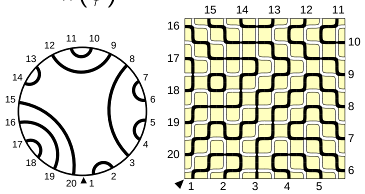

$\pi'(\phi)$

Here's the rule: if the refinement position is odd...

The heretical enumeration

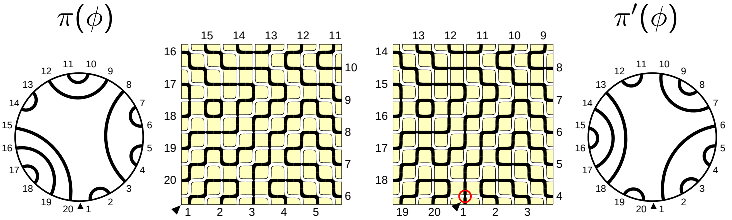

Here's the rule: if the refinement position is odd...

...you just rotate the starting point to the refinement position

The heretical enumeration

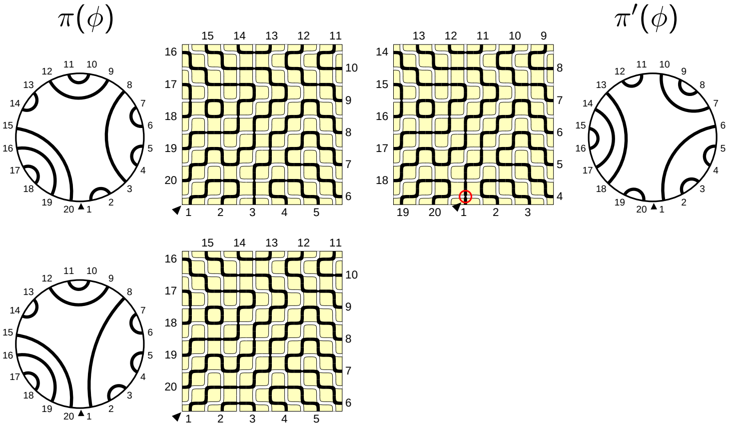

if the refinement position is even...

The heretical enumeration

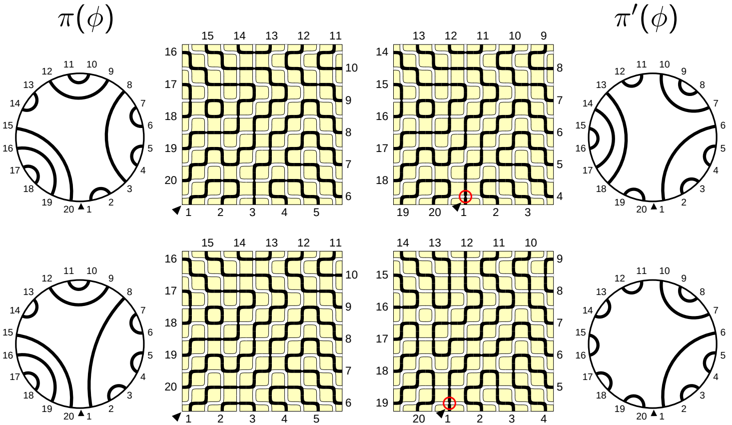

if the refinement position is even...

...you swap black and white, and rotate the starting point

Divide and conqueer

We wanted to prove Di Francesco 2004 conjecture:

$$\mathrm{Sym}\ |\tilde{\Psi}(t)\rangle = \mathrm{Sym}\ |\Psi(t)\rangle$$

with $|\tilde{\Psi}(t)\rangle$ solving $(X_1(t) - R^{-1})|\tilde{\Psi}(t)\rangle = 0$
and $|\Psi(t)\rangle = \sum_{\phi} t^{h(\phi)-1}|\pi(\phi)\rangle$

We have been led to split this in two parts:

$$|\tilde{\Psi}(t)\rangle = |\Psi'(t)\rangle \quad \text{and} \quad \mathrm{Sym}\ |\Psi'(t)\rangle = \mathrm{Sym}\ |\Psi(t)\rangle$$

with $|\Psi'(t)\rangle = \sum_{\phi} t^{h(\phi)-1}|\pi'(\phi)\rangle$

The first relation is proven if you show that

$$(X_1(t) - R^{-1})|\Psi'(t)\rangle \equiv (t\mathbf{1} - R^{-1} - (t-1)e_1)|\Psi'(t)\rangle = 0$$

recalling that $e_1^2 = e_1$, and $(1 - e_1)^2 = (1 - e_1)$:

Divide and conqueer

We wanted to prove Di Francesco 2004 conjecture:

$$\mathrm{Sym}\ |\tilde{\Psi}(t)\rangle = \mathrm{Sym}\ |\Psi(t)\rangle$$

with $|\tilde{\Psi}(t)\rangle$ solving $(X_1(t) - R^{-1})|\tilde{\Psi}(t)\rangle = 0$
and $|\Psi(t)\rangle = \sum_\phi t^{h(\phi)-1}|\pi(\phi)\rangle$

We have been led to split this in two parts:

$|\tilde{\Psi}(t)\rangle = |\Psi'(t)\rangle$ and $\mathrm{Sym}\ |\Psi'(t)\rangle = \mathrm{Sym}\ |\Psi(t)\rangle$
with $|\Psi'(t)\rangle = \sum_\phi t^{h(\phi)-1}|\pi'(\phi)\rangle$

The first relation is proven if you show that

$$(X_1(t) - R^{-1})|\Psi'(t)\rangle \equiv (t\mathbf{1} - R^{-1} - (t-1)e_1)|\Psi'(t)\rangle = 0$$

recalling that $e_1^2 = e_1$, and $(1-e_1)^2 = (1-e_1)$:

Divide and conqueer

We wanted to prove Di Francesco 2004 conjecture:

$$\mathrm{Sym}\ |\tilde{\Psi}(t)\rangle = \mathrm{Sym}\ |\Psi(t)\rangle$$

with $|\tilde{\Psi}(t)\rangle$ solving $(X_1(t) - R^{-1})|\tilde{\Psi}(t)\rangle = 0$
and $|\Psi(t)\rangle = \sum_\phi t^{h(\phi)-1}|\pi(\phi)\rangle$

We have been led to split this in two parts:

$|\tilde{\Psi}(t)\rangle = |\Psi'(t)\rangle$ and $\mathrm{Sym}\ |\Psi'(t)\rangle = \mathrm{Sym}\ |\Psi(t)\rangle$
with $|\Psi'(t)\rangle = \sum_\phi t^{h(\phi)-1}|\pi'(\phi)\rangle$

The first relation is proven if you show that

$$(X_1(t) - R^{-1})|\Psi'(t)\rangle \equiv (t\mathbf{1} - R^{-1} - (t-1)e_1)|\Psi'(t)\rangle = 0$$

recalling that $e_1^2 = e_1$, and $(1 - e_1)^2 = (1 - e_1)$:

Divide and conqueer

We wanted to prove Di Francesco 2004 conjecture:

$$\mathrm{Sym}\ |\tilde{\Psi}(t)\rangle = \mathrm{Sym}\ |\Psi(t)\rangle$$

with $|\tilde{\Psi}(t)\rangle$ solving $(X_1(t) - R^{-1})|\tilde{\Psi}(t)\rangle = 0$
and $|\Psi(t)\rangle = \sum_\phi t^{h(\phi)-1}|\pi(\phi)\rangle$

We have been led to split this in two parts:

$$|\tilde{\Psi}(t)\rangle = |\Psi'(t)\rangle \quad \text{and} \quad \mathrm{Sym}\ |\Psi'(t)\rangle = \mathrm{Sym}\ |\Psi(t)\rangle$$

with $|\Psi'(t)\rangle = \sum_\phi t^{h(\phi)-1}|\pi'(\phi)\rangle$

The first relation is proven if you show that

$$(X_1(t) - R^{-1})|\Psi'(t)\rangle \equiv (t\mathbf{1} - R^{-1} - (t-1)e_1)|\Psi'(t)\rangle = 0$$

recalling that $e_1^2 = e_1$, and $(1 - e_1)^2 = (1 - e_1)$:

$$e_1\ (t\mathbf{1} - R^{-1} - (t-1)e_1)|\Psi'(t)\rangle = 0$$
$$(1 - e_1)\ (t\mathbf{1} - R^{-1} - (t-1)e_1)|\Psi'(t)\rangle = 0$$

Divide and conqueer

We wanted to prove Di Francesco 2004 conjecture:

$$\mathrm{Sym}\ |\tilde{\Psi}(t)\rangle = \mathrm{Sym}\ |\Psi(t)\rangle$$

with $|\tilde{\Psi}(t)\rangle$ solving $(X_1(t) - R^{-1})|\tilde{\Psi}(t)\rangle = 0$
and $|\Psi(t)\rangle = \sum_\phi t^{h(\phi)-1}|\pi(\phi)\rangle$

We have been led to split this in two parts:

$|\tilde{\Psi}(t)\rangle = |\Psi'(t)\rangle$ and $\mathrm{Sym}\ |\Psi'(t)\rangle = \mathrm{Sym}\ |\Psi(t)\rangle$
with $|\Psi'(t)\rangle = \sum_\phi t^{h(\phi)-1}|\pi'(\phi)\rangle$

The first relation is proven if you show that

$$(X_1(t) - R^{-1})|\Psi'(t)\rangle \equiv (t\mathbf{1} - R^{-1} - (t-1)e_1)|\Psi'(t)\rangle = 0$$

recalling that $e_1^2 = e_1$, and $(1-e_1)^2 = (1-e_1)$:

$$e_1\ (\mathbf{1} - R^{-1})|\Psi'(t)\rangle = 0$$
$$(1-e_1)\ (t\mathbf{1} - R^{-1})|\Psi'(t)\rangle = 0$$

FPL in fancy domains...

We considered so far FPL in the $n \times n$ square domain, with alternating boundary conditions,

i.e. consistent fillings of this:

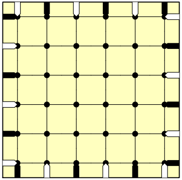

into things like this:

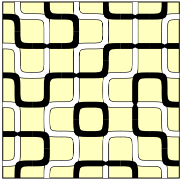

FPL in fancy domains...

We considered so far FPL in the $n \times n$ square domain, with alternating boundary conditions,

i.e. consistent fillings of this:

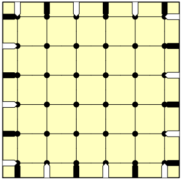

into things like this:

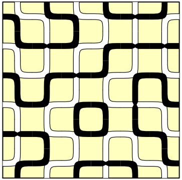

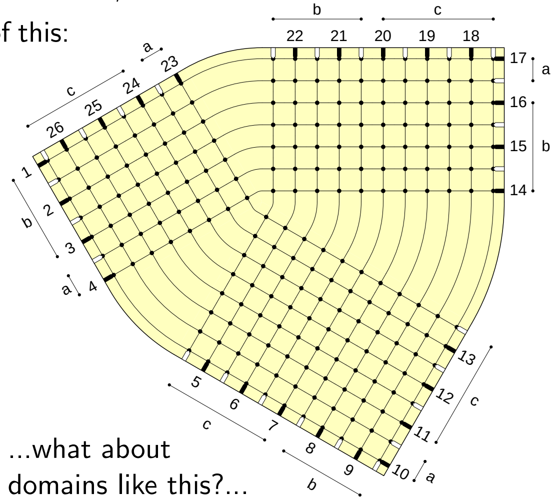

...what about domains like this?...

Fully-Packed Loops in different domains

Let's try to compare enumerations in different domains, with the same perimeter...

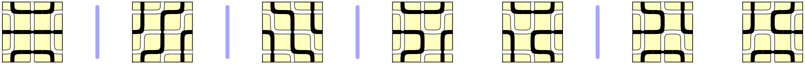

Fully-Packed Loops in different domains

Let's try to compare enumerations in different domains, with the same perimeter...

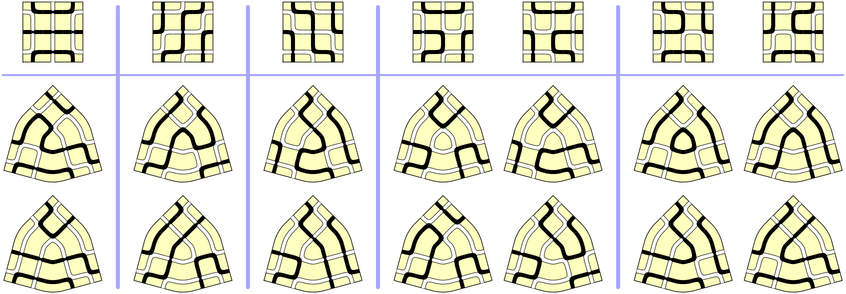

...maybe generalize Razumov–Stroganov before proving it?...

Wieland gyration: the local rules

Say that you have a graph like this:

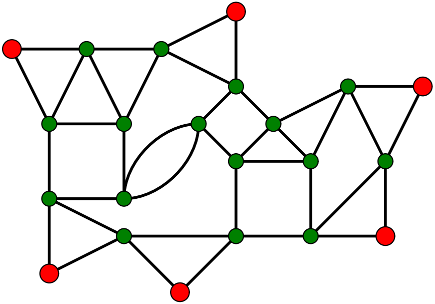

Wieland gyration: the local rules

Say that you have a graph like this:

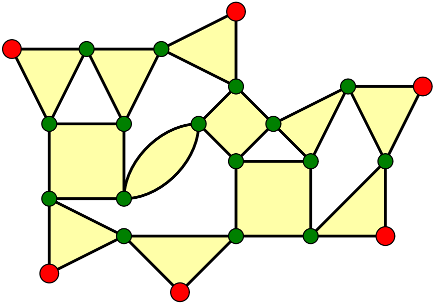

Wieland gyration: the local rules

Given a FPL configuration, you can apply the following involution:

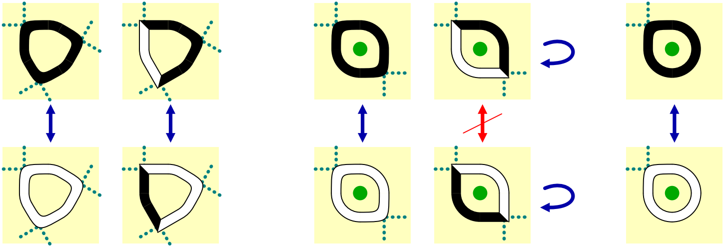

$\ell = 1, 2, 3$

Wieland gyration: the local rules

Given a FPL configuration, you can apply the following involution:

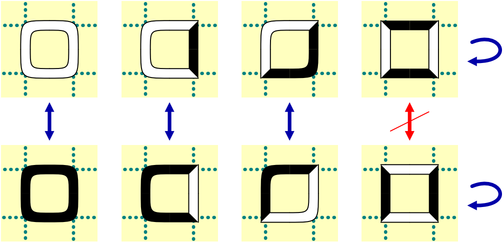

$\ell = 4$

Wieland gyration: the local rules

Given a FPL configuration, you can apply the following involution:

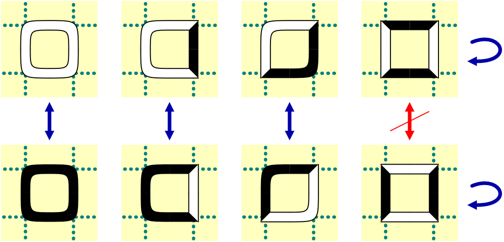

$\ell = 4$

This inverts $\deg_{\text{black}}(v) \leftrightarrow \deg_{\text{white}}(v)$,

and preserves connectivity of open-path endpoints

(and also the way open paths turn around the green punctures)

Wieland gyration: the full picture

...in the original square domain for FPL we have "external legs" (i.e., vertices of degree 1)... if we pair them, to produce triangles, we solve this annoyance...

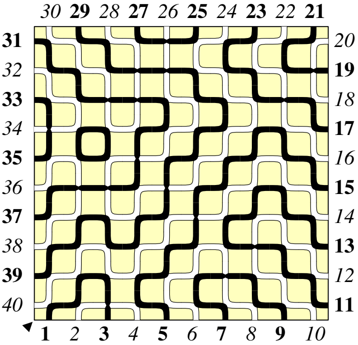

A configuration on (Λ, τ_+)
(i.e., first leg is black)

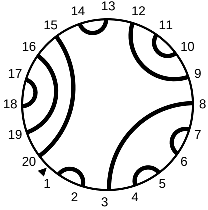

Wieland gyration: the full picture

...in the original square domain for FPL we have "external legs" (i.e., vertices of degree 1)... if we pair them, to produce triangles, we solve this annoyance...

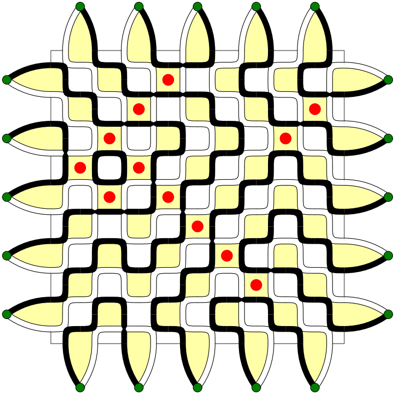

The construction of $\mathcal{G}_+$, pairing $(2j-1, 2j)$ legs (plaquettes are in yellow)

mark in red  and 

Wieland gyration: the full picture

...in the original square domain for FPL we have "external legs" (i.e., vertices of degree 1)... if we pair them, to produce triangles, we solve this annoyance...

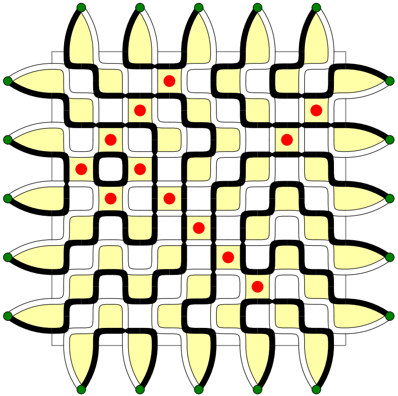

The result of map H_+

Wieland gyration: the full picture

...in the original square domain for FPL we have "external legs" (i.e., vertices of degree 1)... if we pair them, to produce triangles, we solve this annoyance...

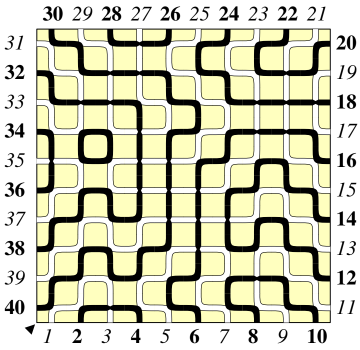

Split auxiliary vertices to recover the (Λ, τ_-) geometry
(i.e., first leg is white)

Wieland gyration: the full picture

...in the original square domain for FPL we have "external legs" (i.e., vertices of degree 1)... if we pair them, to produce triangles, we solve this annoyance...

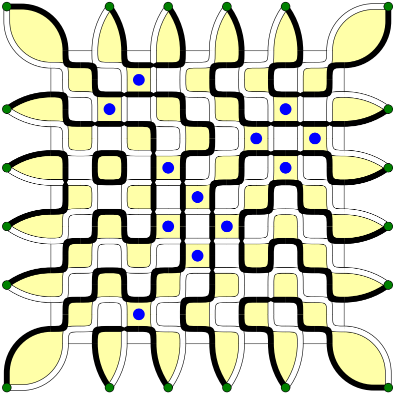

The construction of $\mathcal{G}_-$, pairing $(2j, 2j+1)$ legs

mark in blue  and 

Wieland gyration: the full picture

...in the original square domain for FPL we have "external legs" (i.e., vertices of degree 1)... if we pair them, to produce triangles, we solve this annoyance...

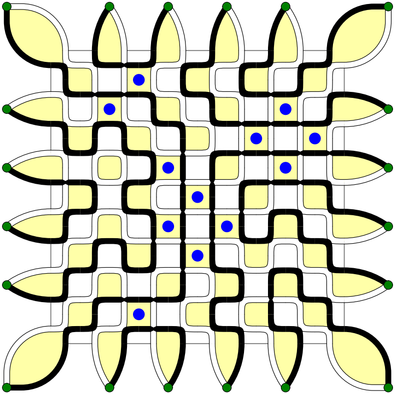

The result of map H_-

Wieland gyration: the full picture

...in the original square domain for FPL we have "external legs" (i.e., vertices of degree 1)... if we pair them, to produce triangles, we solve this annoyance...

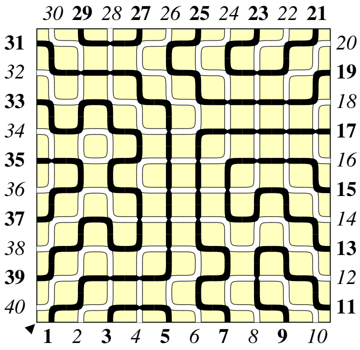

Split auxiliary vertices to recover the (Λ, τ_+) original geometry (with a rotated link pattern)...

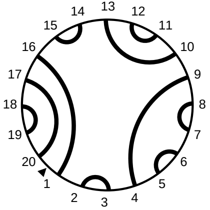

Wieland gyration: where it works

So, the trick is:
- invert $\deg_{\text{black}}(v) \leftrightarrow \deg_{\text{white}}(v)$
- preserve connectivity of open paths

- Works with the Wieland recipe, on faces $\ell = 4$
- Works even more easily on faces $\ell = 1, 2, 3$
- Can't work at all on faces $\ell \geq 5$
- At boundaries, pair external legs to produce triangles

A single move exists on plenty of graphs...

then, rotation comes from two moves

...many more domains than just $n \times n$ squares have this property!

Wieland gyration: where it works

Thus you can trade corners for points of curvature (i.e., faces with less than 4 sides)

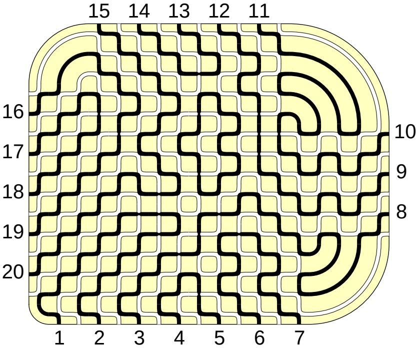

(bottom line: an elementary generalization of Wieland strategy gives rotational symmetry for FPL enumerations above)

Examples of domains with dihedral invariance...

(...and with refined Razumov–Stroganov correspondence...)

1 corner, 3 triangles:

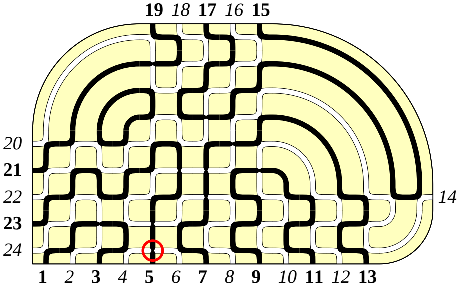

Examples of domains with dihedral invariance...

(...and with refined Razumov–Stroganov correspondence...)

2 corners, 2 triangles:

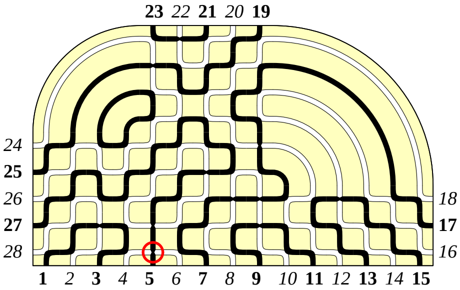

Examples of domains with dihedral invariance...

(...and with refined Razumov–Stroganov correspondence...)

1 corner, 1 face with $\ell = 2$:

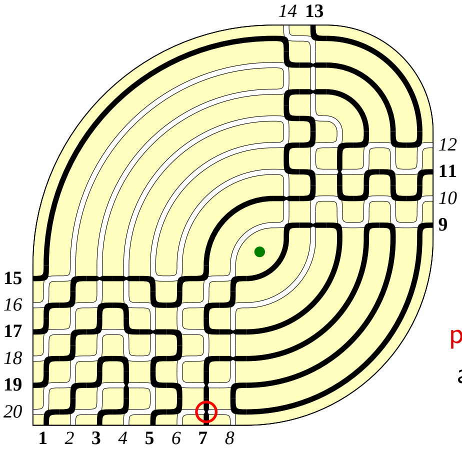

(this works even with punctured link patterns at even sizes, $N = 2n$)

Examples of domains with dihedral invariance...

(...and with refined Razumov–Stroganov correspondence...)

1 corner, 1 degree-2 vertex:

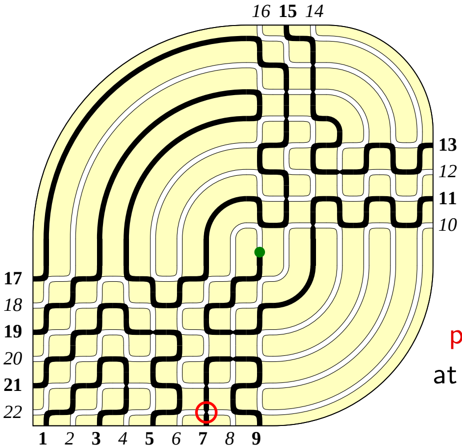

(this works even with punctured link patterns at odd sizes, $N = 2n + 1$)

Examples of domains with dihedral invariance...

(...and with refined Razumov–Stroganov correspondence...)

2 corners, 1 face with $\ell = 2$:
(these are HTASM,
half-turn symmetric ASM's)

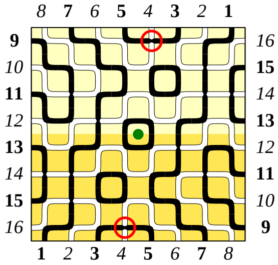

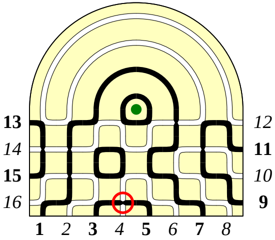

$L = 2n$

Examples of domains with dihedral invariance...

(...and with refined Razumov–Stroganov correspondence...)

2 corners, 1 face with $\ell = 2$:
(these are HTASM,
half-turn symmetric ASM's)

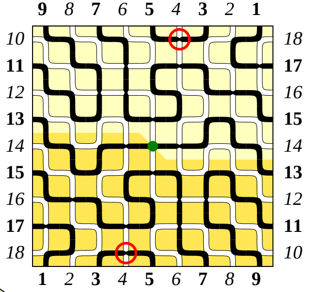

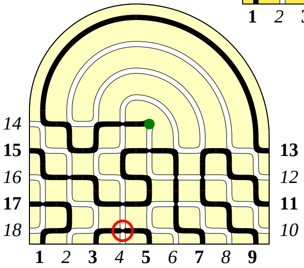

$L = 2n + 1$

Examples of domains with dihedral invariance...

(...and with refined Razumov–Stroganov correspondence...)

2 corners, 1 face with $\ell = 2$:
(these are QTASM,
quarter-turn symmetric ASM's)

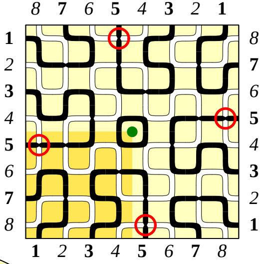

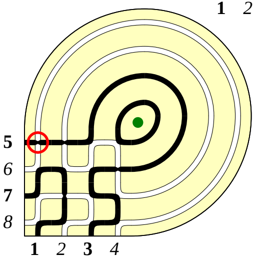

$L = 4n$

Examples of domains with dihedral invariance...

(...and with refined Razumov–Stroganov correspondence...)

2 corners, 1 face with $\ell = 2$:
(these are qQTASM,
quasi–quarter-turn symmetric ASM's)

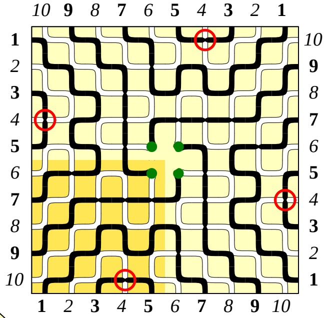

$L = 4n + 2$

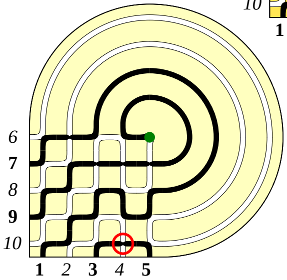

The importance of alternating boundary conditions

We have seen how to generalise the domain,
using black/white alternating boundary conditions

What does it happen if we generalise on boundary conditions?

Pairing consecutive legs with the same colour produces arcs, and "loses link-pattern information": gyration holds for linear combinations of $\Psi(\pi)$, instead of component-wise.

These linear combinations, induced by arcs, are well-described by Temperley-Lieb operators.

We will not need this in full generality...
the study of a single defect is sufficient at our purposes.

Alternating boundary conditions, with one defect

Example: the state $|\Psi^{[j]}\rangle = \sum_{\phi\,:\,h(\phi)=j} |\pi'(\phi)\rangle$ satisfies

$$(R\, e_{j-1} - e_j)|\Psi^{[j]}\rangle = 0$$

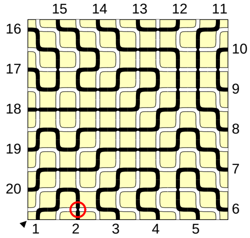

Alternating boundary conditions, with one defect

Example: the state $|\Psi^{[j]}\rangle = \sum_{\phi\,:\,h(\phi)=j} |\pi'(\phi)\rangle$ satisfies

$$(R\, e_{j-1} - e_j)|\Psi^{[j]}\rangle = 0$$

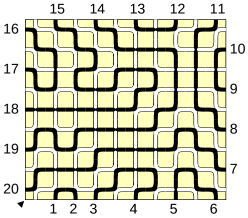

Alternating boundary conditions, with one defect

Example: the state $|\Psi^{[j]}\rangle = \sum_{\phi\,:\,h(\phi)=j} |\pi'(\phi)\rangle$ satisfies

$$(R\, e_{j-1} - e_j)|\Psi^{[j]}\rangle = 0$$

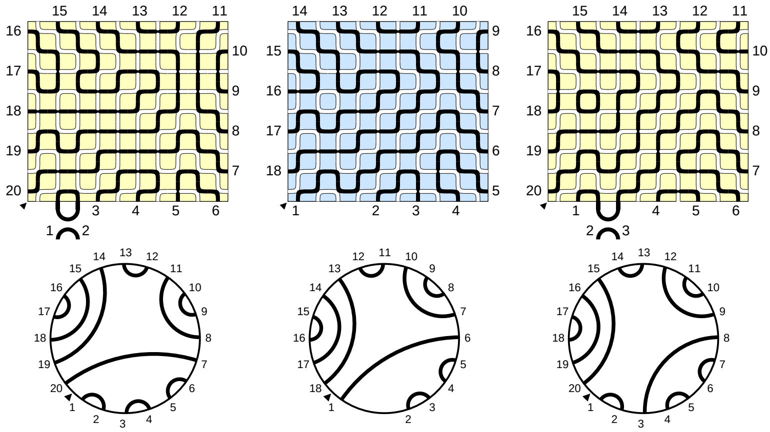

Alternating boundary conditions, with one defect

Example: the state $|\Psi^{[j]}\rangle = \sum_{\phi\,:\,h(\phi)=j} |\pi'(\phi)\rangle$ satisfies

$$(R\, e_{j-1} - e_j)|\Psi^{[j]}\rangle = 0$$

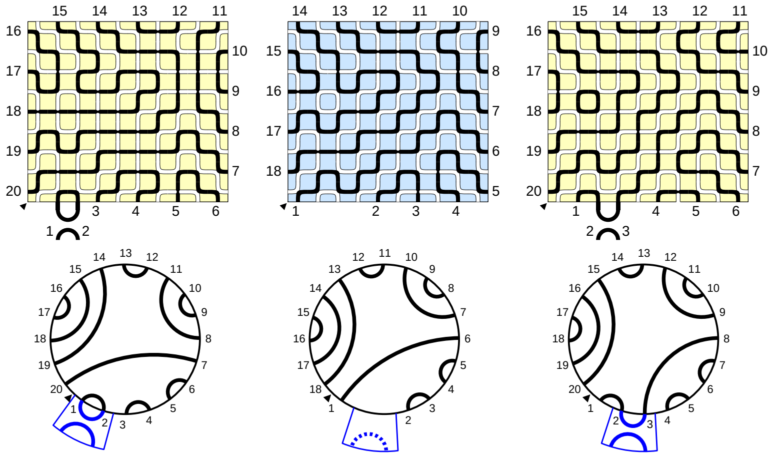

Back to our proof scheme

Recall our checklist of identities:

1 : $e_1\ (\mathbf{1} - R^{-1})|\Psi'(t)\rangle = 0$

2 : $(1 - e_1)\ (t\mathbf{1} - R^{-1})|\Psi'(t)\rangle = 0$

3 : $\mathrm{Sym}\ |\Psi'(t)\rangle = \mathrm{Sym}\ |\Psi(t)\rangle$

(2) is equivalent to ask that $t\Psi(t;\pi) = \Psi(t; R^{-1}\pi)$, for all π such that $1 \not\sim 2$...

but this is easily seen: $1 \not\sim 2$ forces a small region, that in turns implies a simple behaviour of the refinement position under gyration

Back to our proof scheme

Recall our checklist of identities:

1 : $e_1\,(\mathbf{1} - R^{-1})|\Psi'(t)\rangle = 0$ ✔ We have just proven this!

2 : $(1 - e_1)\,(t\mathbf{1} - R^{-1})|\Psi'(t)\rangle = 0$

3 : $\mathrm{Sym}\,|\Psi'(t)\rangle = \mathrm{Sym}\,|\Psi(t)\rangle$

(2) is equivalent to ask that $t\Psi(t;\pi) = \Psi(t;R^{-1}\pi)$, for all π such that $1 \not\sim 2$...

but this is easily seen: $1 \not\sim 2$ forces a small region, that in turns implies a simple behaviour of the refinement position under gyration

Back to our proof scheme

Recall our checklist of identities:

1 : $e_1\ (\mathbf{1} - R^{-1})|\Psi'(t)\rangle = 0$ ✔ We have just proven this!

2 : $(1 - e_1)\ (t\mathbf{1} - R^{-1})|\Psi'(t)\rangle = 0$

3 : $\mathrm{Sym}\ |\Psi'(t)\rangle = \mathrm{Sym}\ |\Psi(t)\rangle$ ➽ Look at gyration even better!

(2) is equivalent to ask that $t\Psi(t;\pi) = \Psi(t; R^{-1}\pi)$,
for all π such that $1 \not\sim 2$...

but this is easily seen: $1 \not\sim 2$ forces a small region, that in turns implies a simple behaviour of the refinement position under gyration

Back to our proof scheme

Recall our checklist of identities:

1 : $e_1\,(\mathbf{1} - R^{-1})|\Psi'(t)\rangle = 0$ ✔ We have just proven this!

2 : $(1 - e_1)\,(t\mathbf{1} - R^{-1})|\Psi'(t)\rangle = 0$

3 : $\mathrm{Sym}\,|\Psi'(t)\rangle = \mathrm{Sym}\,|\Psi(t)\rangle$ ➽ Look at gyration even better!

(2) is equivalent to ask that $t\Psi(t;\pi) = \Psi(t; R^{-1}\pi)$,
for all π such that $1 \not\sim 2$...

but this is easily seen: $1 \not\sim 2$ forces a small region, that in turns implies a simple behaviour of the refinement position under gyration

Back to our proof scheme

Recall our checklist of identities:

1 : $e_1\ (\mathbf{1} - R^{-1})|\Psi'(t)\rangle = 0$ ✔ We have just proven this!

2 : $(1 - e_1)\ (t\mathbf{1} - R^{-1})|\Psi'(t)\rangle = 0$ ✔

3 : $\mathrm{Sym}\ |\Psi'(t)\rangle = \mathrm{Sym}\ |\Psi(t)\rangle$ ➽ Look at gyration even better!

(2) is equivalent to ask that $t\Psi(t;\pi) = \Psi(t; R^{-1}\pi)$,
for all π such that $1 \not\sim 2$...

but this is easily seen: $1 \not\sim 2$ forces a small region, that in turns implies a simple behaviour of the refinement position under gyration

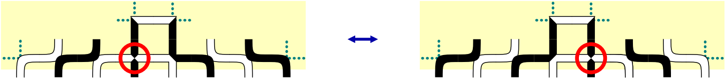

Back to our proof scheme

Recall our checklist of identities:

1 : $e_1\,(\mathbf{1} - R^{-1})|\Psi'(t)\rangle = 0$ ✔ We have just proven this!

2 : $(1 - e_1)\,(t\mathbf{1} - R^{-1})|\Psi'(t)\rangle = 0$ ✔

3 : $\mathrm{Sym}\,|\Psi'(t)\rangle = \mathrm{Sym}\,|\Psi(t)\rangle$ ➽ Look at gyration even better!

(2) is equivalent to ask that $t\Psi(t;\pi) = \Psi(t;R^{-1}\pi)$,
for all π such that $1 \not\sim 2$...

but this is easily seen: $1 \not\sim 2$ forces a small region, that in turns implies a simple behaviour of the refinement position under gyration

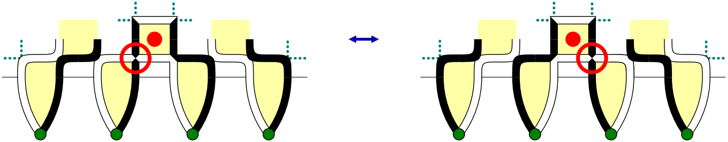

And now for something completely different. . .

The Razumov–Stroganov correspondence exists also in a second version, involving FPL with a reflection symmetry and the $O(1)$ Dense Loop Model on a strip with a boundary.

This *should* have been a variant of the just-proven case with dihedral symmetry. . . however, our proof approach does not work! (and the conjecture is open at present)

Vertical Razumov–Stroganov Conjecture

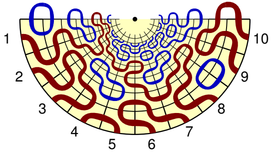

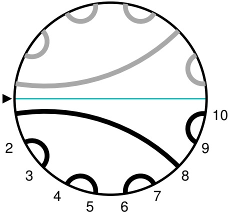

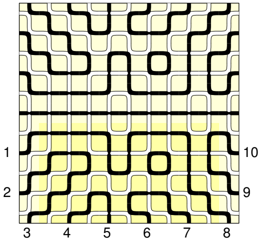

$\tilde{\Psi}_n(\pi)$: probability of π
in the $O(1)$ Dense Loop Model
in the $\{1, \ldots, n\} \times \mathbb{N}$ strip

$\Psi_n(\pi)$: probability of π
for vertically-symmetric FPL
with uniform measure in the
$(n+1) \times (n+1)$ square

Vertical Razumov–Stroganov Conjecture

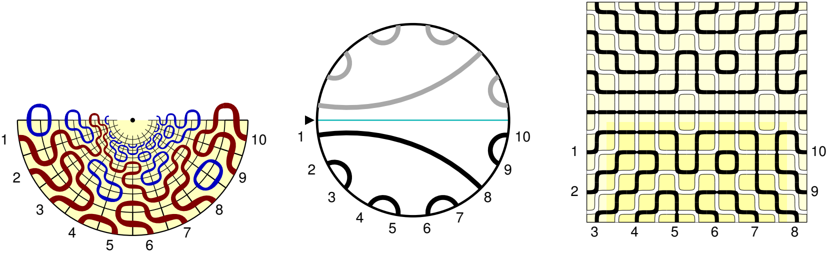

$\tilde{\Psi}_n(\pi)$: probability of π
in the $O(1)$ Dense Loop Model
in the $\{1, ..., n\} \times \mathbb{N}$ strip

$\Psi_n(\pi)$: probability of π
for vertically-symmetric FPL
with uniform measure in the
$(n+1) \times (n+1)$ square

Razumov–Stroganov conjecture – vertical case

$$\tilde{\Psi}_n(\pi) = \Psi_n(\pi)$$

Domains with vertical Razumov–Stroganov correspondence

In the case of the dihedral Razumov–Stroganov correspondence, understanding the appropriate family of domains has been a crucial ingredient

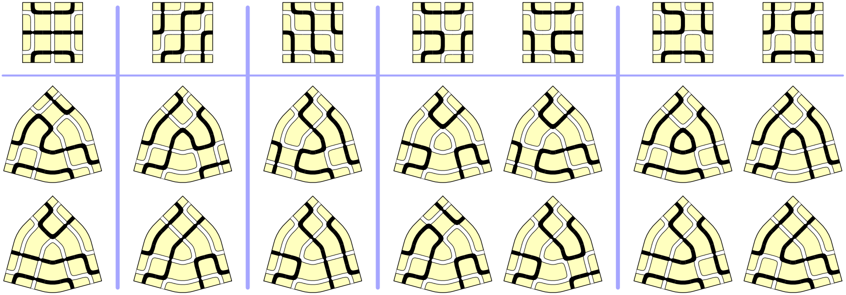

Domains with vertical Razumov–Stroganov correspondence

In the case of the dihedral Razumov–Stroganov correspondence, understanding the appropriate family of domains has been a crucial ingredient

We think we know how to do this also in the vertical case, and even with up to two boundary parameters (at the two sets of U-turns)

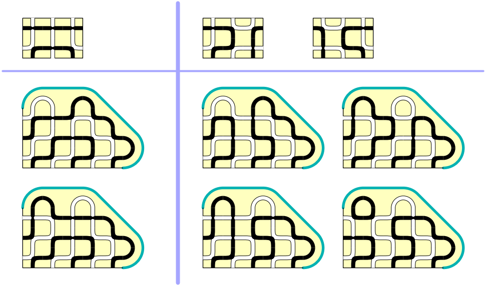

$3 + x + 7y + 2xy + 4y^2 + xy^2$ $\qquad$ $6 + 2x + 14y + 4xy + 8y^2 + 2xy^2$

Some bibliography

David P. Robbins,
The story of 1, 2, 7, 42, 429, 7436,... Math. Intelligencer, 1991

David M. Bressoud,
Proofs and Confirmations: The Story of the Alternating-Sign Matrix Conjecture, (Math. Ass. of America, 1999)

Paul Zinn-Justin,
Six-vertex, loop and tiling models: integrability and combinatorics,
`arXiv:0901.0665` (Lambert Ac. Publ., 2010)

Luigi Cantini and Andrea Sportiello,
Proof of the Razumov–Stroganov conjecture,
`arXiv:1003.3376` J. Comb. Theory series A **118** (2011) 1549-1574
A one-parameter refinement of the Razumov–Stroganov correspondence,
`arXiv:1202.5253` *to appear in J. Comb. Theory series A*

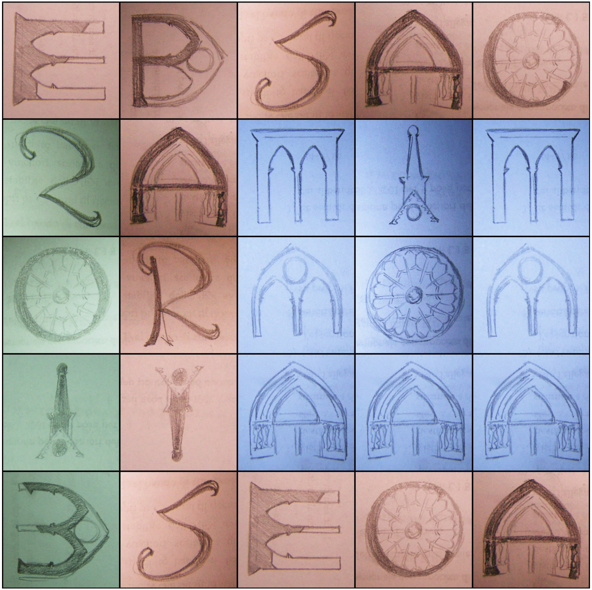

Merci !

End of the talk (extra material follows...)

A final observation on the orbits

Consider the orbits under Wieland half-gyration
As FPL in the same orbit have the same link pattern up to rotation, $\mathrm{Sym}\, |\Psi'(t)\rangle = \mathrm{Sym}\, |\Psi(t)\rangle$ follows if, for every j, and every orbit, there are as many contributions t^{j-1} to $|\Psi'(t)\rangle$ as to $|\Psi(t)\rangle$.

Study the behavior of the trajectory $h(x)$ of the refinement position:

- $h(x+1) - h(x) \in \{0, \pm 1\}$
- In a periodic function, a height value is attained alternately on ascending and descending portions (if not at maxima/minima)
- All maxima/minima plateaux have length 2,
  the rest has slope ± 1
- Ascending/descending parts of the trajectory have respectively black and white refinement position

A final observation on the orbits

Consider the orbits under Wieland half-gyration
As FPL in the same orbit have the same link pattern up to rotation, $\mathrm{Sym}\,|\Psi'(t)\rangle = \mathrm{Sym}\,|\Psi(t)\rangle$ follows if, for every j, and every orbit, there are as many contributions t^{j-1} to $|\Psi'(t)\rangle$ as to $|\Psi(t)\rangle$.

Study the behavior of the trajectory $h(x)$ of the refinement position:

- $h(x+1) - h(x) \in \{0, \pm 1\}$
- In a periodic function, a height value is attained alternately on ascending and descending portions (if not at maxima/minima)
- All maxima/minima plateaux have length 2,
  the rest has slope ± 1
- Ascending/descending parts of the trajectory have respectively black and white refinement position

A final observation on the orbits

As a consequence, in any orbit O, and for any value j, the numbers of $\phi \in O$ such that $h(\phi) = j$, and

- are in even (resp. odd) position in the orbit;
- or have a black (resp. white) refinement position;

are all equal. This completes the proof.

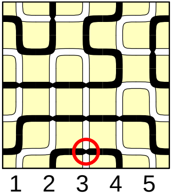

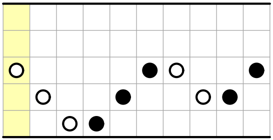

A final observation on the orbits

As a consequence, in any orbit O, and for any value j, the numbers of $\phi \in O$ such that $h(\phi) = j$, and

- are in even (resp. odd) position in the orbit;
- or have a black (resp. white) refinement position;

are all equal. This completes the proof.

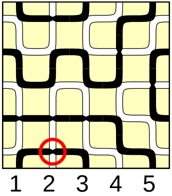

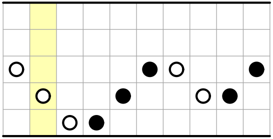

A final observation on the orbits

As a consequence, in any orbit O, and for any value j, the numbers of $\phi \in O$ such that $h(\phi) = j$, and

- are in even (resp. odd) position in the orbit;
- or have a black (resp. white) refinement position;

are all equal. This completes the proof.

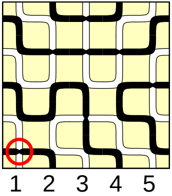

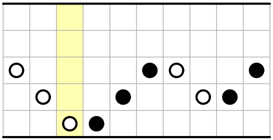

A final observation on the orbits

As a consequence, in any orbit O, and for any value j, the numbers of $\phi \in O$ such that $h(\phi) = j$, and

- are in even (resp. odd) position in the orbit;
- or have a black (resp. white) refinement position;

are all equal. This completes the proof.

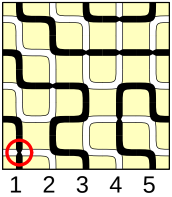

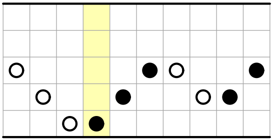

A final observation on the orbits

As a consequence, in any orbit O, and for any value j, the numbers of $\phi \in O$ such that $h(\phi) = j$, and

- are in even (resp. odd) position in the orbit;
- or have a black (resp. white) refinement position;

are all equal. This completes the proof.

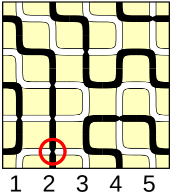

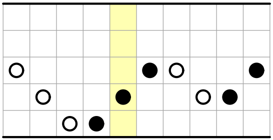

A final observation on the orbits

As a consequence, in any orbit O, and for any value j, the numbers of $\phi \in O$ such that $h(\phi) = j$, and

- are in even (resp. odd) position in the orbit;
- or have a black (resp. white) refinement position;

are all equal. This completes the proof.

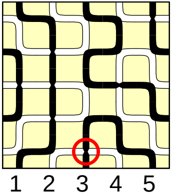

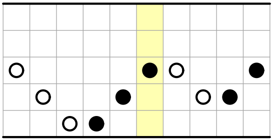

A final observation on the orbits

As a consequence, in any orbit O, and for any value j, the numbers of $\phi \in O$ such that $h(\phi) = j$, and

- are in even (resp. odd) position in the orbit;
- or have a black (resp. white) refinement position;

are all equal. This completes the proof.

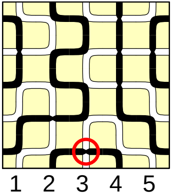

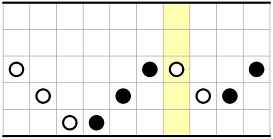

A final observation on the orbits

As a consequence, in any orbit O, and for any value j, the numbers of $\phi \in O$ such that $h(\phi) = j$, and

- are in even (resp. odd) position in the orbit;
- or have a black (resp. white) refinement position;

are all equal. This completes the proof.

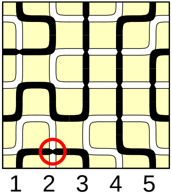

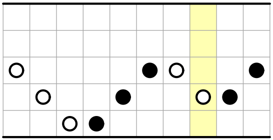

A final observation on the orbits

As a consequence, in any orbit O, and for any value j, the numbers of $\phi \in O$ such that $h(\phi) = j$, and

- are in even (resp. odd) position in the orbit;
- or have a black (resp. white) refinement position;

are all equal. This completes the proof.

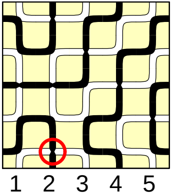

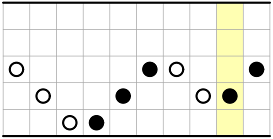

A final observation on the orbits

As a consequence, in any orbit O, and for any value j, the numbers of $\phi \in O$ such that $h(\phi) = j$, and

- are in even (resp. odd) position in the orbit;
- or have a black (resp. white) refinement position;

are all equal. This completes the proof.